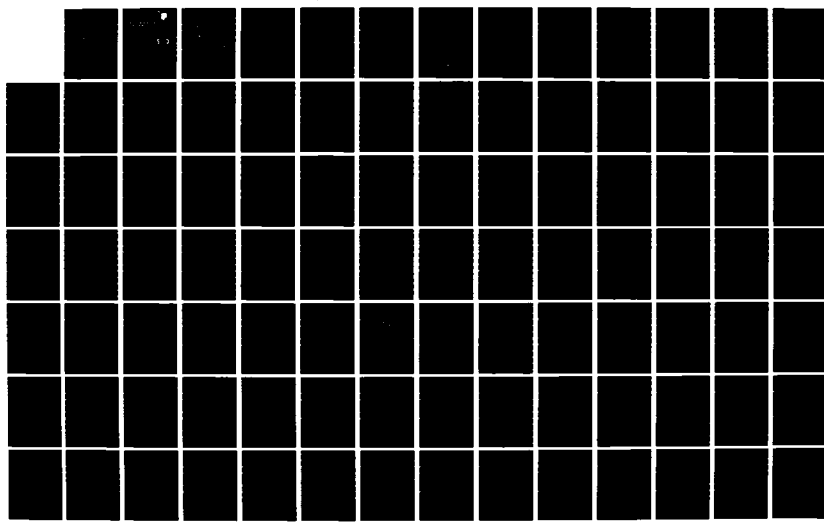


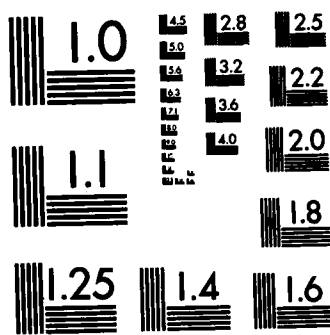
AD-A123 530 ACROSS FIFTEEN (ACTIVE CONTROL OF SPACE STRUCTURES) (U) 1/2
CONTROL DYNAMICS CO HUNTSVILLE AL S M SELTZER ET AL.
OCT 82 RADC-TR-82-198 F30602-81-C-0179

UNCLASSIFIED

F/G 22/2

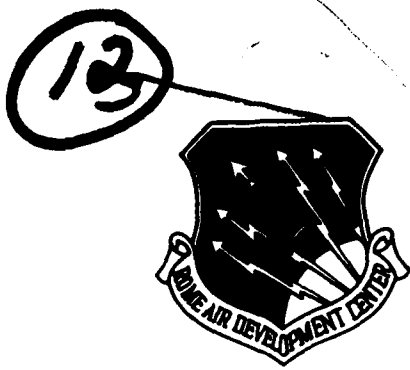
NL





MICROCOPY RESOLUTION TEST CHART
NATIONAL BUREAU OF STANDARDS-1963-A

RADC-TR-82-198
Final Technical Report
October 1982



ACROSS FIFTEEN (ACTIVE CONTROL OF SPACE STRUCTURES)

AD A 123530

Control Dynamics Company

Sponsored by
Defense Advanced Research Projects Agency (DOD)
ARPA Order No. 3654

13
DTIC
ELECTE
S JAN 19 1983 D
B

APPROVED FOR PUBLIC RELEASE; DISTRIBUTION UNLIMITED

The views and conclusions contained in this document are those of the authors and should not be interpreted as necessarily representing the official policies, either expressed or implied, of the Defense Advanced Research Projects Agency or the U.S. Government.

**ROME AIR DEVELOPMENT CENTER
Air Force Systems Command
Griffiss Air Force Base, NY 13441**

DTIC FILE COPY

This document has been reviewed by the RADC Public Affairs Office (PA) and
the Defense Technical Information Service (DTIS). It will be made available to the general public, including foreign nations.

REF ID: A22102-170 has been reviewed and is approved for publication.

APPROVED:



RICHARD W. CAIRNS
Project Engineer

APPROVED:



FRANK J. QUINN
Technical Director
Surveillance Division

FOR THE COMMANDER:



JOHN P. ROSS
Acting Chief, Plans Office

If your address has changed or if you wish to be removed from the RADC
mailing list, or if the addressee is no longer employed by your organization,
please notify RADC (OCSE) Griffiss AFB NY 13441. This will assist us in
maintaining a current mailing list.

Do not return copies of this report unless contractual obligations or notices
on a specific document requires that it be returned.

ACOSS FIFTEEN (ACTIVE CONTROL OF SPACE STRUCTURES)

Sherman M. Seltzer
Eugene H. Worley
Randy J. York

Contractor: Control Dynamics Company
Contract Number: F30602-81-C-0179
Effective Date of Contract: 15 April 1981
Contract Expiration Date: 1 May 1982
Short Title of Work: ACOSS FIFTEEN (Active Control of Space
Structures)
Program Code Number: 1E20
Period of Work Covered: Apr 81 - May 82

Principal Investigator: Sherman M. Seltzer
Phone: (205) 539-8111

Project Engineer: Richard W. Carman
Phone: (315) 330-3148

Approved for public release; distribution unlimited.

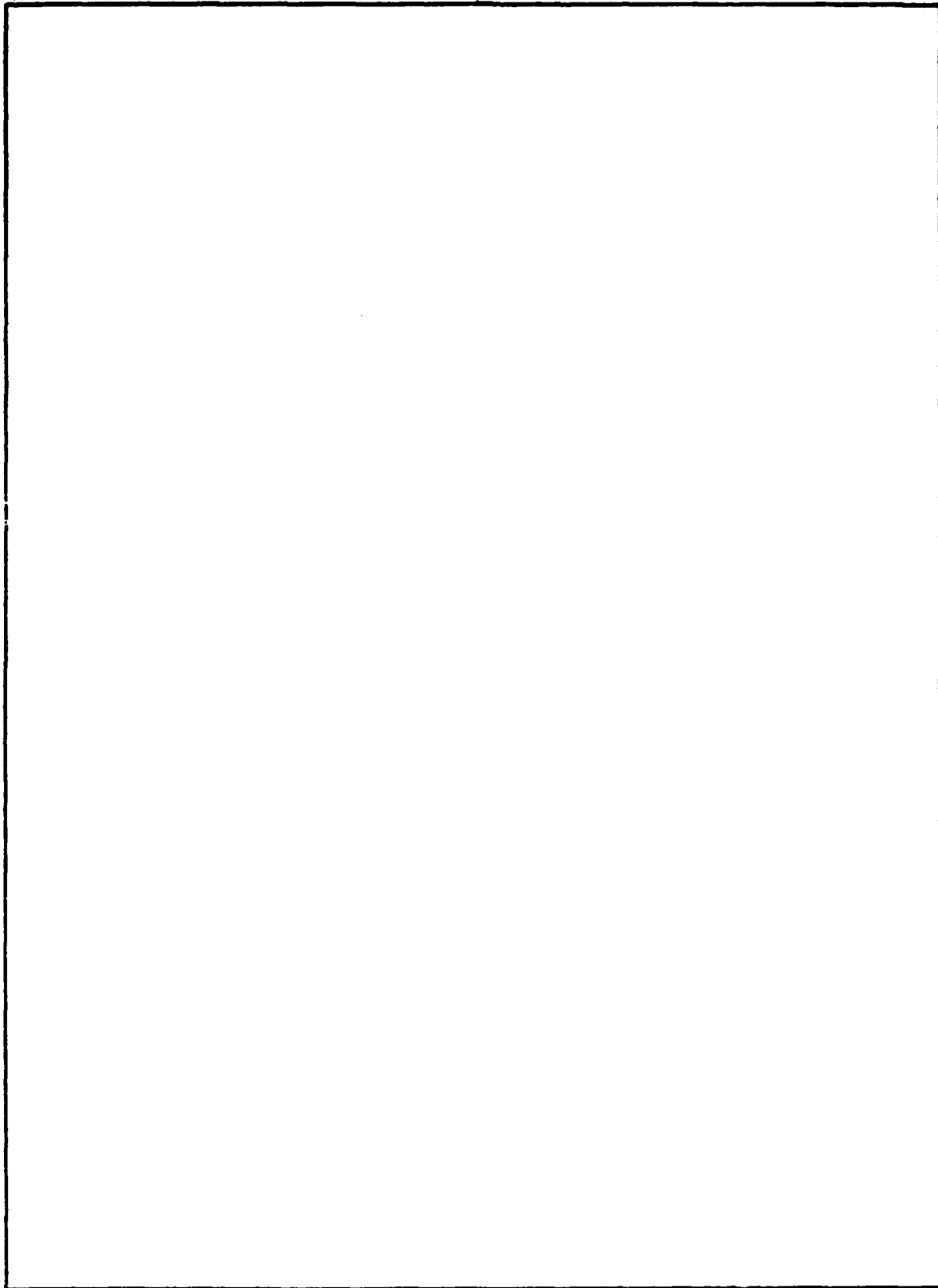
This research was supported by the Defense Advanced Research
Projects Agency of the Department of Defense and was monitored
by Richard W. Carman (RADC/OCSE) Griffiss AFB NY 13441 under
Contract F30602-81-C-0179.

UNCLASSIFIED

SECURITY CLASSIFICATION OF THIS PAGE (When Data Entered)

UNCLASSIFIED

SECURITY CLASSIFICATION OF THIS PAGE(When Data Entered)



UNCLASSIFIED

SECURITY CLASSIFICATION OF THIS PAGE(When Data Entered)

ACKNOWLEDGEMENT

The work reported upon in this report was performed by the Control Dynamics Company of Huntsville, Alabama under Contract No. F30602-81-C-0179. It was supported by the Department of Defense Advanced Research Projects Agency (DARPA) and monitored by Rome Air Development Center. The DARPA Program Manager is LTC Allen F. Herzberg, USAF, and the Rome Air Development Center Project Engineer is Mr. Richard Carman.

The Program Manager and Principal Investigator is Dr. Sherman M. Seltzer. and the Co-Investigator is Dr. H. Eugene Worley.

Accession For	
NTIS GRA&I	<input checked="" type="checkbox"/>
DTIC TAB	<input type="checkbox"/>
Unannounced	<input type="checkbox"/>
Justification	
By _____	
Distribution/ _____	
Availability Codes _____	
Dist	Avail and/or Special
A	



TABLE OF CONTENTS

1.0	INTRODUCTION	1
1.1	Objective	1
1.2	Scope	1
1.3	Statement of Work	2
1.4	Schedule	7
1.5	Contract Implementation	9
2.0	VCOSS FLEXIBLE APPENDAGE MODELING	10
3.0	DEVELOPMENT OF DIGITAL CONTROL ANALYSIS TECHNIQUES . .	11
4.0	STABILITY OF LARGE SCALE SYSTEMS	29
5.0	CONCLUSIONS	47
6.0	DISTRIBUTION LIST	48
APPENDIX	DARPA-WPAFB VCOSS DYNAMIC MODEL	ATTACHED

1.0 INTRODUCTION

1.1 OBJECTIVE

→ To study active structure control technology as applied to Large Space Structures (LSS). In particular, to develop analysis and design techniques for utilization of practicing control system engineers in their investigations of future Large Space Structures (LSS). These techniques will be "use" qualified through application to a representative model of a LSS. This objective is in support of the overall ACOSS objective which is to develop and understand a generic, unified structural dynamics and control technology base for LSS with stringent Line-Of-Sight (LOS) and figure performance requirements that must be maintained in the presence of onboard and natural disturbances.

1.2 SCOPE

→ This effort will be restricted to theory development, experiment design, demonstration and documentation of structural dynamics and control technology for large precision spacecraft. The contractor shall plan the overall effort, define the problem, develop and evaluate solutions. The development and evaluation of solutions will involve analytical studies, modeling and simulations. The contractor shall identify and document all the analyses, studies, designs, models, simulations, tradeoffs, issues, software, requirements, specifications and data produced under the contract. Important products of the effort will be the demonstration and documentation of new control technology.

1.3 STATEMENT OF WORK

The following four tasks comprise the original Statement of Work. Task 1 has been deferred for implementation in ACOSS-17. The content was subsequently modified to incorporate Tasks 5 - 7 to support the VCOSS (Vibration Control of Space Structures) Program.

1.3.1 ORIGINAL TASK/TECHNICAL REQUIREMENTS

Task 1 - Investigation of Structural Damping Models: Investigate the problem of how to accurately represent structural modal damping for a structure that is subjected to disturbance and control forces. Structures with values of critical damping of less than 2% can be adequately described by assuming equivalent viscous modal damping coupled with real eigenvectors. However, for larger amounts of damping these assumptions do not appear to be true. Investigate this problem in depth and develop a complete understanding of the proper form and implementation of structural damping for use in the analysis and development of active control technology for LSS.

Develop a mathematical model containing discrete viscous damping at related modes throughout the structure.

Compare the response of the discrete viscous damping model to that of an identical model containing modal rather than discrete equivalent viscous damping.

Develop a mathematical model with an accurate form of structural damping (proportional to displacement and at a 90 degrees phase angle) followed by comparison of the response with the models developed above.

Task 2 - Development of Digital Control Analysis Techniques: Investigate sampling phenomena arising from a digital version of an onboard controller, using a truncated version of the model developed by the contractor under Contract F30602-81-C-0179. Give special emphasis to the effects of "folding" of the higher neglected modal bending frequencies into the control system bandwidth. Establish design criteria so that onboard computer sampling rates can be selected and the appropriate tradeoffs can be made.

Task 3 - Flexible Appendage Model: Perform and document modifications of the transfer matrix technique for simple structures with rigid appendages that are applicable to LSS. Include extensions of the technique that contain flexible appendages. The resulting equations shall be documented with their attendant computer program implementations.

Task 4 - Stability of Large Scale Systems: Use the decomposition principle that was applied under Contract F30602-81-C-0179 to stabilize a preliminary LSS model and apply it to the higher fidelity models that are being developed under Tasks 2 and 3.

Oral Presentations: Oral presentations shall be given at such times and places as designated by the Contracting Officer. Sufficient notices will be provided prior to any briefing.

1.3.2 "VCOSS" TASKS/TECHNICAL REQUIREMENTS

Task 5 - Develop requirements for LSS models: Determine system characteristics. Assimilate the system level requirements into a format and set useable by a Structural Analyst to provide the basis for an accurate and reliable structural model.

Develop derived control system requirements. Structure the system level requirements in the form of derived requirements as viewed by a Controls Analyst. This shall include, but not be limited to, the specification of potential sensor and actuator locations and the limitations on the structural natural frequency, if any.

Determine the form of the structural models. Review the requirements developed above, both system and derived control, and determine the appropriate technique to be applied to the models. A Lagrangian approach shall be investigated. It may not be used if, when compared with other techniques, it proves to be inferior in terms of taking full advantage of modern high speed computer technology and maximizing the degree of understanding and "feel" of the expected results.

Task 6 - Develop "stiff" structural model: Develop mass and stiffness matrices. Develop mass and stiffness matrices for the candidate structure using the techniques and procedure in Task 5. Develop a model with sufficient degrees of freedom and fidelity to meet contemporary LSS specifications.

Develop structural characteristics. Derive the structural characteristics (eigenvalues and eigenvectors) for all significant modes of the required model. Develop the structural gains at all possible sensor, actuator, and disturbance locations. If multiple paths are required (as in multiple reflections of mirror surfaces), then the modal gains associated with these shall also be developed.

Task 7 - Develop "flexible" structural model: Develop mass and stiffness matrices. Develop the mass and stiffness matrices for the candidate structure using the technique and procedure determined under Task 5. Develop a model with sufficient degrees of freedom and fidelity to meet the contemporary LSS specifications.

Determine eigenvalues and vectors. Derive the structural characteristics (eigenvalues and eigenvectors) for all significant mods of the required model.

Develop the structural gains at all possible sensor, actuator, and disturbance locations. If multiple paths are required, as in multiple reflections off mirror surfaces, then the modal gains associated with these shall be developed.

1.4 SCHEDULE

The original scheduled duration of the contract was the twelve month period beginning 15 April 1981. As a result of the VCOSS modification, the VCOSS Final Report (incorporated within this Final Report) was delivered (with an oral report) prior to 30 December 1981. The ACOSS-15 Final Presentation was delivered to LTC Herzberg (DARPA) and Mr. Carman (RADC) on 28 April 1982 in Huntsville, Alabama. A compilation of due dates and deliverable items comprises Table I.

TABLE I. DUE DATES AND STATUS OF DELIVERABLE ITEMS

<u>DATE</u>	<u>ITEM</u>
1 June 1981	* R&D Status #1 * ACROSS 15 Schedule * ACROSS 15 Milestones/WBS
1 July 1981	* R&D Status #2
1 August 1981	* R&D Status #3
1 September 1981	* R&D Status #4
1 October 1981	* R&D Status #5
1 November 1981	* R&D Status #6
1 December 1981	* R&D Status #7
1 January 1982	* R&D Status #8
1 February 1982	* R&D Status #9
1 March 1982	* R&D Status #10
1 April 1982	* R&D Status #11
1 May 1982	* R&D Status #12 * Final Oral Presentation * Final Technical Report * Abstract of New Technology

1.5 CONTRACT IMPLEMENTATION

Dr. Seltzer was the Principal Investigator for the ACOSS-15. He also performed the Task 2.

Dr. Worley and Dr. Glaese performed the main effort performing Tasks 3, 5, 6, and 7.

Dr. York performed the main effort concerning Task 4.

The effort associated with Task 1 was deferred for performance under ACOSS-17.

2.0 VCOSS FLEXIBLE APPENDAGE MODELING

Tasks 3 ("Flexible Appendage Model"), 5 ("Develop requirements for LSS models"), 6 ("Develop 'stiff' structural model"), and 7 ("Develop 'flexible' structural model") are reported upon in one cohesive appendix. This appendix is a report entitled "DARPA-WPAFB VCOSS Dynamic Model" and was presented to DARPA and Wright Patterson AFB personnel (as well as Lockheed and TRW ACOSS contractor personnel) on 1 October 1981.

The report presents analysis results applied to a model developed for DARPA by the Charles Stark Draper Laboratory. The analysis technique embodies a combination of finite element modeling, closed-form solutions of continuous beams, and modal synthesis. The advantages of this approach are that detailed modeling can be applied where necessary while still retaining the ability to make modifications and changes with a minimum of effort and elapsed time.

3.0 DEVELOPMENT OF DIGITAL CONTROL ANALYSIS TECHNIQUE

The purpose of this section is to describe an integrated analytical approach to the development of digital control systems. This philosophy includes the dynamic effects of sampling phenomena early in the design development. Further it attempts to enhance computer simulation efficiency by incorporating analysis tools to prescribe numerical values for system parameters and to predict simulation results. The main body of this section was presented at the IEEE EASCON in Washington, D.C. on November 18, 1981.

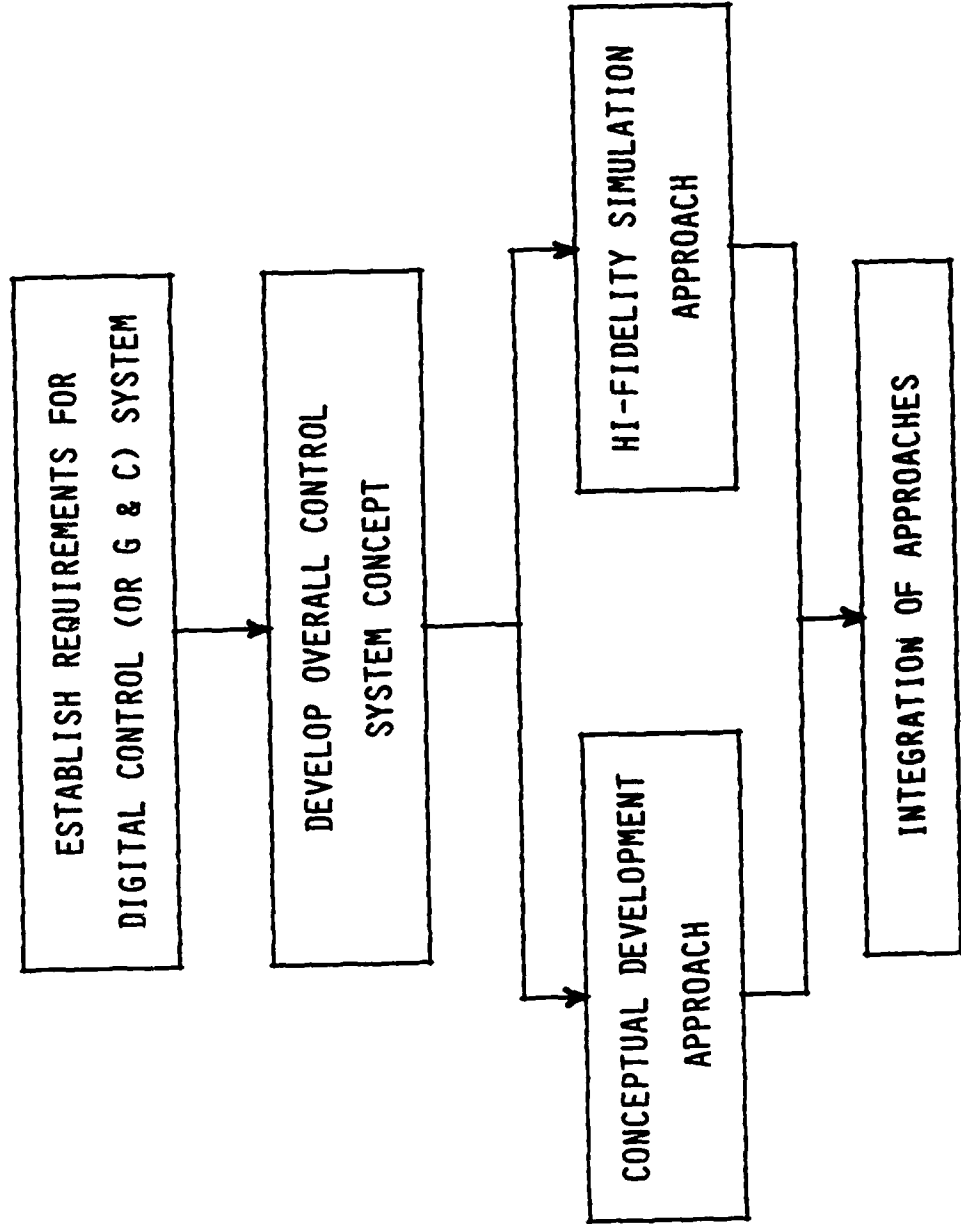
The design philosophy espoused in this section takes advantage of high-fidelity, high-order digital simulation tools coupled with low order analysis techniques that permit mathematical tractability. After describing that philosophy, the major portion of the section is devoted to a description of three analytical digital design tools and how they can be used in concert. These tools are: (1) the Systematic Analytical Method (SAM) which is a method for obtaining mathematical relationships between desired system inputs and system outputs; (2) the Cross-Multiplication Method which provides a means of obtaining the time-domain response from the system closed-loop transfer function; and (3) the Digital Parameter Space Method which permits one to examine and specify the dynamics of a system. The use of these tools together is demonstrated in a simple example.

Since the preponderance of control system theory has been developed from the standpoint of linear and continuous systems, the design analysis process usually starts with the assumption that the system is continuous and not digitally sampled. Thus, the intrinsic quality of digital computation, namely sampling, tends to be ignored until the last design step at which point one typically says, "Well, we'll simply sample 'fast enough' so that it doesn't make any difference". However, as the control system becomes more complex and additional requirements arise, the capability to sample "fast enough" may not be available. In addition, the designer must answer the question, "What is fast enough?"

In this section it will be demonstrated that the sampling phenomena can be included in the early stages of the design process to yield valuable information regarding not only control system design requirements but vehicle configuration requirements as well.

The design philosophy may be described graphically in Fig. 3-1. Each block of the figure will be described below.

FIG. 3-1 "A DESIGN PHILOSOPHY"



3.1. REQUIREMENTS AND SYSTEM CONCEPT

First, the requirements for the digital control system must be clearly set forth. This trivial and innocuous-appearing step is often overlooked or poorly performed, contributing to great quantities of subsequent pain (to the designers) and sometimes poor performance. After the requirements have been specified, an overall control system concept is developed. At this point in time, two parallel approaches may be initiated: The high-fidelity simulation approach and the conceptual development approach.

3.2. HIGH-FIDELITY SIMULATION APPROACH

This usually begins in the form of a finite element model of the overall system. The outputs of this model are usually in the form of eigenvalues and eigenvectors. [The real part of each eigenvalue represents the square of the respective modal frequency (in units of rad/s), and the corresponding eigenvector represents the modal displacement for each of the included degrees of freedom (normalized to a unit generalized mass).] The outputs of the finite element model, i.e. the modal descriptions, are then used in the development of a high-fidelity, high-order computer simulation. The simulation can be all-digital or can begin in that form and evolve to a simulation that includes hardware-in-the-loop¹.

3.3 CONCEPTUAL DEVELOPMENT APPROACH

In this approach, the system concept is simplified into an analytically tractable model. This model is then analyzed to gain an understanding of its dynamics in detail. It also has the purpose of providing numerical values for system parameters (e.g., control gains, sampling periods, etc.) to use in the high-order computer simulation. Once these initial goals have been achieved, the fidelity (and complexity) of the model is gradually increased. Ultimately, the dynamic performance of this model is compared with that of the high-order simulation to predict the latter's character and hence assist in the "de-bugging" the program. If dynamic agreement does not accrue, then the order of the simplified model is increased further until agreement is achieved.

Concurrent with the development of the simplified analytical model, a simplified structural model is developed. The purpose of this structural model is to provide the simplified analytical model developer with modal characteristics in a timely manner. Of course, if it is felt that modal characteristic will be forthcoming from the finite element model in a timely (with respect to the control system designer's simplified analytical model needs) manner, then development of the simplified structural model is not needed. (In the author's design experience, this timeliness has never been demonstrated.)

Once the simplified models have been completed integrated, they are used in the development of a time-response computer model. The purpose of this model is to verify the overall flow and compatibility of the control system concept. Since time-invariant coefficients are assumed in the differential and difference equations used when the simplified analytical design tools are applied, the simulation provides a valuable check of the validity of these assumptions during simulated operation.

3.4 INTEGRATION OF THE TWO APPROACHES

The overall control system concept is the point of initiation of the two approaches, which are developed in parallel. As numerical values are developed for system parameters in the "Conceptual Development Approach," they are integrated into the "High-Fidelity Simulation Approach" development. Further, the dynamic response and performance determined by using the simplified models are then compared with the responses of the high-order simulation (and its various subordinate portions) to assist in "de-bugging" the simulation.

3.5 SIMPLIFIED DESIGN TOOLS

The primary design tools used in the "Conceptual Design Approach" are:

- * The Systematic Analysis Method (SAM). This is a method for obtaining mathematical relationships between desired system inputs and system outputs. These relationships may then be used to investigate and prescribe desired transient and steady state system performance characteristics (by applying, for instance, the Digital Parameter Space Method and the Final Value Theorem). They may also be used to determine the system response in the time-domain (by applying, for instance, the Cross-Multiplication Method). The SAM technique is described below.
- * The Cross-Multiplication Method. This is a technique for obtaining the response of a digitally-controlled system from its closed-loop transfer function. Since this technique has already been described in a similar IEEE conference, it will only be described herein.²
- * The Digital Parameter Space Method. This technique may be used to examine and specify the dynamics of the digitally-controlled system. Briefly it permits one to map the locations of the roots of the system characteristic equation into a space whose coordinates are the system's free parameters. It is similar to a multi-dimensional root locus plot. This method (or any other method the control system designer chooses) is used to determine the system parameters and digital computer sampling period. Because the technique is described in the literature, it will only be summarized in this paper.³

3.5.1 SYSTEMATIC ANALYTICAL METHOD (SAM)

SAM is implemented by performing the following four steps. If the equations resulting from the first three steps are placed in a table of three columns (one for each step), they are easily manipulated to perform the fourth and final step.

1. Step No. 1 Obtain "System Equations"

First one selects as unknowns the variables at the inputs to each of the samplers in the system. The original equations describing the system are rewritten in the Laplace domain and tabulated. If the system is already described by a block diagram, the "system equations" may be written upon inspection.

2. Step No. 2 Obtain "Modified System Equations"

If any of the "system equations" contain terms that consist of the product of any unsampled system variable and an unsampled transfer function, they must be modified by substitution to eliminate the unsampled variables. For orderliness, these modified equations are also tabulated (in the same rows as their respective original equations).

3. Step No. 3 Obtain "Pulsed System Equations"

Pulse transforms are now taken of each side of the "modified system equations," yielding "pulsed system equations." If the asterick (*) is used to denote the ideal impulse sampling phenomenon, then the transformation into the sampled domain is performed according to the relationships,

$$(R) * = R* \quad (\text{III-1})$$

$$(RG) * = \overline{RG*} \quad (\text{III-2})$$

$$(RG*) * = R*G* \quad (\text{III-3})$$

4. Step No. 4 Obtain Desired Input/Output Relationships

All system variables, both pulsed and continuous, may be found in either the "system equations" (Step No. 1) or the "pulsed system equations" (Step No. 3). The desired output(s) may be solved for by solving the appropriate "system" or "pulsed system" equations, substituting as necessary.

The pulsed (starred) forms of the variables and transfer functions may all be transformed into the z-domain by noting that the z-transform of the variable (or transfer function) $C^*(s)$ is merely $C(z)$, using standard digital

nomenclature.⁴ (Recall, $z=e^{sT}$, where s is the complex Laplace operator and T represents the digital sampling period.) If it is desired to find an output expression in modified z-transform form (so that the system response ultimately can be determined at any instant of time), that may also readily be accommodated. Suppose a pulsed variable, C^* , is equal to the product of an unstarred quantity (such as a transfer function), $A(s)$, and a starred quantity (such as an input variable), $B^*(s)$, i.e.

$$C^*(s) = A(s,m) B(s) \quad (\text{III-4})$$

where $A(s)$ or $B^*(s)$ may be equal to unity. The modified z-transform may always be obtained from Eq. (III-4) by performing the transformation:

$$C(z,m) = A(z,m) B(z) \quad (\text{III-5})$$

where $A(z,m)$ represents the modified z-transform of the quantity $A(s)$, and $B(z)$ represents the ordinary z-transform of the quantity $B(s)$.⁴ This technique appears to be an attractive alternative to obtaining modified z-transforms through Signal Flow Graph techniques (which may of course be done).

3.5.2.4 SYSTEM RESPONSE BY CROSS-MULTIPLICATION METHOD²

Once the relationship between the desired output and the desired input has been established (e.g. by Step No. 4 of SAM) in the pulsed (starred) form and transformed into the z or modified z-domain, that relationship may be expressed as a ratio of two polynomials in z (or modified z, if desired). For example, if the desired output is denoted as C(z) and the desired input is denoted as R(z), their relationship in the z-domain may be written as

$$\frac{C(z)}{R(z)} = \frac{\sum_{j=0}^M a_j z^j}{\sum_{k=0}^N b_k z^k} \quad (\text{III-6})$$

where coefficients a_j and b_k represent the system parameters. As demonstrated in Reference 2, the procedure for finding the response, C, in the time domain merely consist of three steps. First one crossmultiplies the numerators on each side of Eq. (III-6) by the denominator. Then each term of the resulting expression is divided by the expression, $b_N z^N$. Finally, the Real Translation Theorem* is applied to that result, yielding values of the desired response at each sampling instant nT , i.e.

$$c(nT) = \frac{1}{b_N} \left\{ \sum_{j=0}^M a_j r(n - N + j)T - \sum_{k=0}^N b_k c(n - N + k) T \right\} \quad (\text{III-7})$$

where j, k, M, N , and n are integers.

If it is desired to find the intra-sampling response, it may be accomplished by applying either the Submultiple Method or the Modified z-Transform Method. Both techniques are merely modest extensions of the above-described Cross-Multiplication Method and are described in Ref. 2.

3.5.3 DIGITAL PARAMETER SPACE METHOD³

Briefly, the method permits one to map the locations of the roots of the system's characteristic equation onto a plane (or three-space, if desired) whose coordinates are the system's free parameters. In addition to the characteristic root locations, such things as contours of constant relative damping ratios (ζ) and specified exponential time constant may be portrayed as contours on the parameter space. Thus in a manner somewhat reminiscent of the classical root locus method, a portrait may be presented of all pertinent aspects of the system's transient response as functions of several parameters (rather than the single parameter, open-loop gain).

3.5.4 EXAMPLE

A simplified model of a typical satellite system is shown in Figure 3-2. The associated system equations of motion may be written in vector-matrix notation by applying SAM. The unknowns are selected to be the inputs to the samplers, i.e. $e(t)$. Applying Step No. 1 of SAM, the equations of motion for these two unknowns plus the system output, $x(t)$, may be written as:

$$X = G_p F G_{ho} U^* \quad (\text{III-8})$$

$$U = D E^* \quad (\text{III-9})$$

$$E = R - Y = R - C X \quad (\text{III-10})$$

Capital letters are used in Eqs. (III-8) - (III-16) to denote matrices and vectors, and asterisks (throughout the paper) represent impulse (i.e. ideal or perfect) sampling. These equations may be tabulated as the first column of the Table. Next, Step No. 2 of SAM is applied to Eqs. (III-8) - (III-10) to obtain the "modified system equations", i.e.

$$X = G_p F G_{ho} U^* \quad (\text{i.e., no change}) \quad (\text{III-8})$$

$$U = D E^* \quad (\text{no change}) \quad (\text{III-9})$$

$$E = R - Y = R - (C G_p F G_{ho}) U^* \quad (\text{III-10})$$

Equations (III-8), (III-9), and (III-10) may be placed in column 2 of the Table. Next Step No. 3 is applied to these equations to obtain the corresponding "pulsed system equations" (which may be placed in column 3 of the Table):

$$X^* = (G_p G G_{ho})^* U^* \quad (\text{III-12})$$

$$U^* = D^* E^* \quad (\text{III-13})$$

$$E^* = R^* - Y^* = R^* - (C G_p F G_{ho})^* U^* \quad (\text{III-14})$$

Finally, Step No. 4 may be applied to obtain the relationship between the system pulsed output, X^* , and the referenced pulsed input, R^* , by substituting Eq. (III-14) into Eq. (III-13) and then substituting the resulting equation into Eq. (III-12), ultimately yeilding

$$X^* = \overline{G_p F G_{ho}}^* D^* R^* (I + D^* \overline{C G_p F G_{ho}}^*)^{-1} \quad (\text{III-15})$$

where I represents the identity matrix. The z-transform of each side of Eq. (III-15) may be taken to yield

$$X(z) = \overline{G_p F G_{ho}}(z) D(z) R(z) [I + D(z) \overline{C G_p F G_{ho}}(z)]^{-1} \quad (\text{III-16})$$

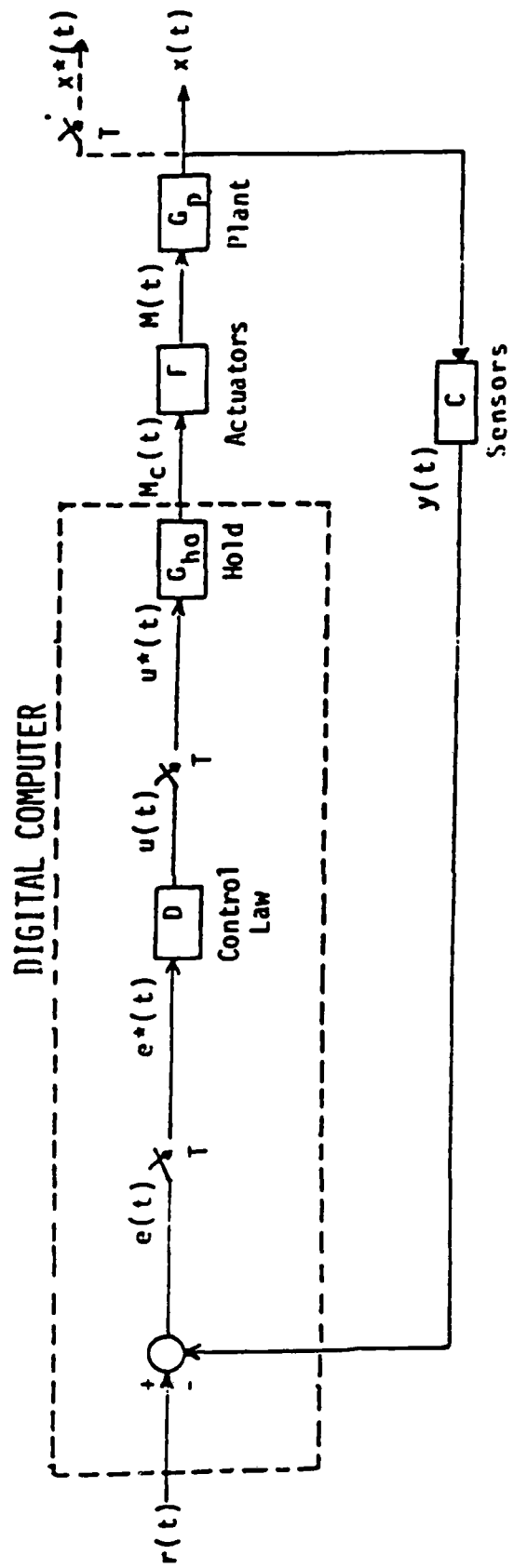


FIGURE 3-2
SIMPLIFIED ATTITUDE CONTROL SYSTEM

A digital proportional integral differential (PID) controller may be postulated. If the integration operation is approximated by the trapezoidal approximation,

$$D_T(z) = \frac{T(z+1)}{2(z-1)} \quad (\text{III-17})$$

The PID controller $D(z)$ may be written as

$$D(z) = \frac{U(z)}{E(z)} = K_p D_T(z) + K_i D_T^2(z) + K_d \quad (\text{III-18})$$

$$= \frac{\frac{1}{2}K_p T(z^2 - 1) + \frac{1}{4}K_i T^2 (z-1)^2 + K_d (z-1)^2}{(z-1)^2}$$

If one defines A_p , A_i , A_d as

$$A_p = \frac{d}{dt} \left[\frac{1}{2}K_p T^2 / J \right], A_i = \frac{d}{dt} \left[\frac{1}{4}K_i T^3 / J \right], A_d = \frac{d}{dt} [K_d T / J] \quad (\text{III-19})$$

one may readily obtain the closed-loop transfer function described by Eq. (III-20) and Table 3-1:

$$\frac{X(z)}{R(z)} = \frac{\sum_{j=0}^2 d_j z^j}{\sum_{j=0}^3 g_j z^j} \quad (\text{III-20})$$

Table 3-1: CLTF Coefficients

j	d_j	g_j
0	$-A_p + A_i + A_d$	$d_0 - 1$
1	$2(A_i - A_d)$	$d_1 + 3$
2	$A_p + A_i + A_d$	$d_2 - 3$
3	---	1

The closed-loop transfer function of Eq. (III-20) can now be used to determine both the steady-state and the transient behavior of the system. Further, the Cross-Multiplication Method may be applied to Eq. (III-20) to determine the time-domain response of the system.

The form of the controller selected can be checked, in a coarse sense, by determining the system steady state response to an expected form of disturbance. This can be done by applying the Final Value Theorem to Eq. (III-20) after substituting the z-domain version of the reference input into that equation and solving for $\dot{\theta}$. If a typical reference input is a unit step function, for example, then

$$\dot{\theta}_c(z) = z/(z-1). \quad (\text{III-21})$$

Substituting Eq. (III-21) into Eq. (III-20), solving for $\dot{\theta}(z)$, and finally applying the Final Value Theorem⁶ to the result, one obtains the steady state value for $\dot{\theta}(t)$:

$$\lim_{t \rightarrow \infty} \dot{\theta}(t) = \lim_{z \rightarrow 1} \{(1-z^{-1})(\dot{\theta}_c(z)) \cdot (\dot{\theta}(z)/\dot{\theta}_c(z))\} = 1 \quad (\text{III-22})$$

Not unexpectedly, this is the desired value in the steady state.

One may now solve for the time response of the system by applying the Cross-Multiplication Method to Eq. (III-20), yielding

$$\dot{\theta}(k) = \left\{ \begin{array}{l} (A_p + A_i)\dot{\theta}_c(k-1) + 2A_i\dot{\theta}_c(k-2) \\ -(A_p - A_i)\dot{\theta}_c(k-3) - (A_p + A_i - A_d - 3)\dot{\theta}(k-1) \\ -(2A_i - 2A_d + 3)\dot{\theta}(k-2) + (A_p - A_i - A_d + 1)\dot{\theta}(k-3) \end{array} \right\} \quad (\text{III-23})$$

where the symbol $\dot{\theta}(k)$ represents the value of $\dot{\theta}(kT)$ at the k th value of T , i.e. at the time instant $k=kT$. Note that the difference equation (III-23) can admit any initial conditions and that the form of the reference input, $\dot{\theta}_c(kT)$, need not be specified except at the sampling instants (i.e. it can be complicated in form or even irrational).

Finally, the numerical values of the control system gains and the sampling period, T , may be specified with the aid of the Parameter Space Method. Because it has been amply described in the literature, only a final form of a parameter plane is shown. An example of the use of this technique is briefly shown. The denominator of the closed-loop transfer function, Eq. (III-20), becomes the system characteristic equation when set equal to zero.

The stability boundaries from the z-domain are mapped onto a selected parameter space in A_D , A_p , A_I ; the plane of the paper defines the $A_D - A_p$ space (see Figure III-3). The $z=+1$ boundary is defined by the plane $A_p=0$, and the $z=-1$ boundary by the plane $A_D=2$. The $z=e^{j\omega nT}$ boundary is a surface, the contours of which are defined by curves designated by their associated numerical values of A_I (as A_I varies from 0 to 1.4).

Contours associated with various values of damping ratio (ζ) are then mapped onto the same space (Figure III-4), as are lines associated with various values of real root locations (δ). Since the characteristic equation is third order, one would expect the space to be spanned by intersections of contours indicating locations of three roots. For example, at the suggested design point, one pair of complex conjugate roots has a damping ratio of 0.707 and the real root is located at approximately 0.1. From this frequency domain information the system dynamics can be deduced in terms of the system gains (parameters) and sampling period (T). The actual time domain response is then found by using the Cross-Multiplication Method to produce an appropriate difference Eq. (III-23), inserting the numerical values associated with the candidate design point selected on the parameter space. Using this equation, the system response to various forms of reference inputs can then be determined explicitly for various choices of gains of sampling period.

REFERENCES

1. Pastrick, H.L. & Seltzer, S.M., "A Validated Methodology for Accurately Prediction Missile Flight Performance," Paper AAS 81-004, American Astronautical Society Annual Rocky Mountain Guidance and Control Conference, Keystone, CO, Jan. 31-Feb. 4, 1981.
2. Seltzer, S.M., "Determination of Digital Control System Response by Cross-Multiplication," Conference Proceedings IEEE Southeastcon '81, Huntsville, AL, April 5-8, 1981, pp.621-623
3. Seltzer, S.M., "Application of the Parameter Space Method to Aerospace Digital Control System Design," IEEE Transactions on Automatic Control, Vol. AC-26, No. 2, April 1981, pp 530-533
4. Kuo, B.C., Analysis and Synthesis of Sampled Data Control Systems, Englewood, NJ, Prentice-Hall, 1963.

Control Dynamics Company
PARAMETER SPACE

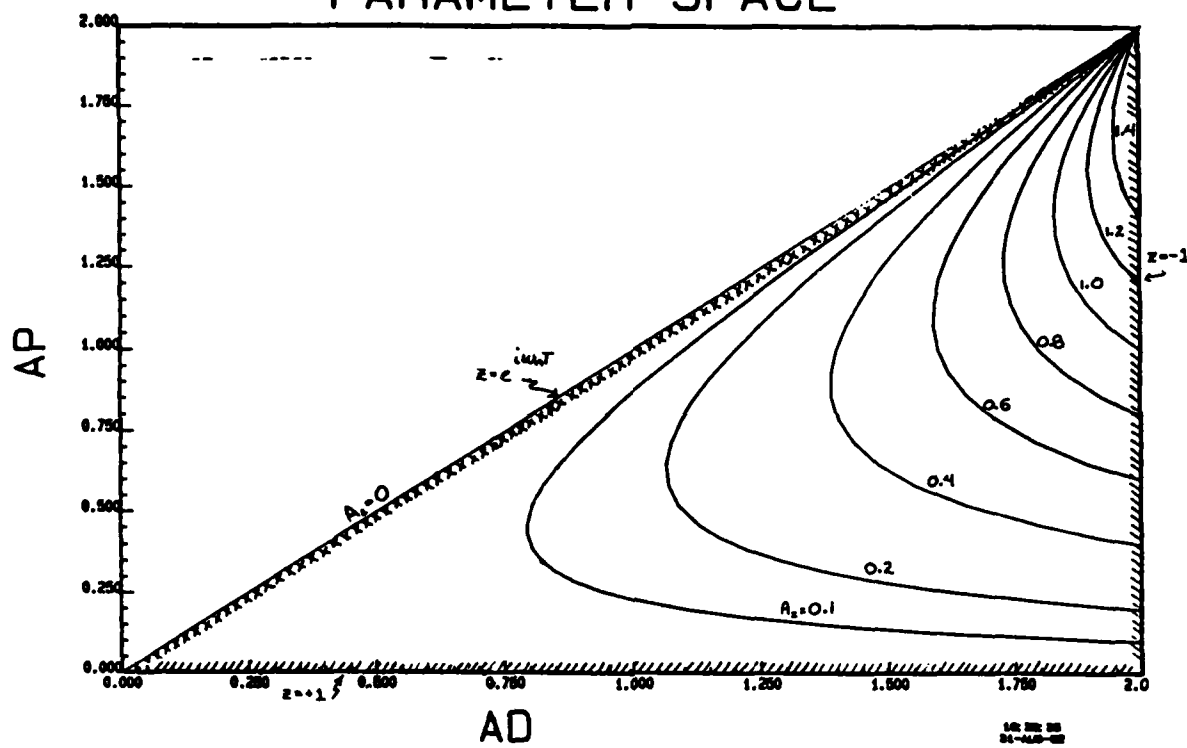
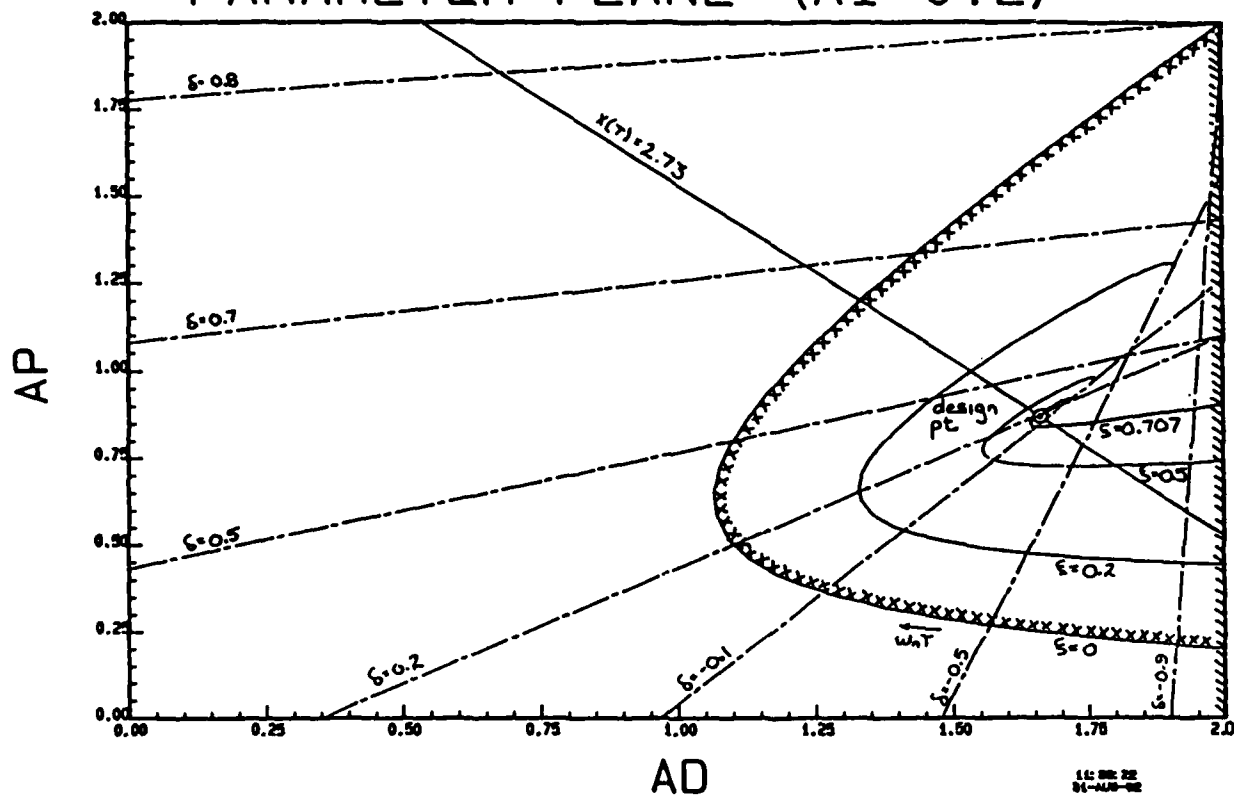


FIGURE III - 3 STABILITY

Control Dynamics Company
 PARAMETER PLANE ($A_I = 0.2$)



PARAMETER PLANE ($A_I = 0.2$)
 FIGURE III-4

CANDIDATE DESIGN PT: $A_p = 0.87$, $A_I = 0.2$, $A_D = 1.66$
 $\omega_M T = 1.93$, $\xi = 0.707$, $\delta = 0.1$
 $X(T) = A_p + A_I + A_D = 2.73$
 $X(2T) = 0.55$

4.0 STABILITY OF LARGE SCALE SYSTEMS

4.1 INTRODUCTION

The problem attacked in this section is to develop a method to determine stability regions of feedback control gains for a large scale DARPA type system, such as that described in Section 2.0. The approach is to extend the parameter space technique for discrete control systems to permit inclusion of an arbitrary number of bending modes. The large scale system will be represented in modal coordinates, and the discrete feedback controller will employ both attitude (θ) and attitude rate ($\dot{\theta}$). The problem will be to find the respective control gains K_p and K_d (see Figure 4-1) that will insure stability. The resulting algorithm to yield the required form of the system characteristic equation must be suitable for computer implementation and simulation.

It is assumed that the digital onboard controller will be of the position/derivative of position (PD) form. The two parameters selected for portrayal on the parameter plane are K_p and K_d . For the simplified example, only one sensor and one torquer are used, and colocation is not assumed.

4.2 PARAMETER SPACE METHOD

Based primarily on the work of D. D. Siljak,¹ the parameter space method is an analytical tool developed for use in control system analysis and synthesis. Briefly, the method as developed by S. M. Seltzer,² permits one to map the location of the roots of the system's characteristic equation onto a plane (or three-space if desired) whose coordinates are the system's free parameters. The characteristic equation must be of the form,

$$C. E. = \sum_{i=1}^M [A_i k_0 + B_i k_1 + F_i] z^i \quad (4-1)$$

The plane is readily divided into regions identified with system stability and instability. The method can then be used to provide a graphical display of stability regions for two specified parameters, such as k_0 and k_1 . The free parameters need not be gains but just as well could be other system parameters. In addition to the characteristic root locations, other factors of interest such as constant damping ratios and specified exponential time constant may

be portrayed as contours on the parameter space. Thus in a manner somewhat reminiscent of the classical root locus method, a portrait may be presented of all pertinent aspects of the system's transient response as functions of several parameters (rather than the single parameter, open-loop gain), and as a function of the independent argument, ωT , where ω is the system damped frequency and T is the digital sampling period. An automated generation of the arrays A, B, and F for an arbitrary number (M) of bending modes is highly desirable, where

$$\begin{aligned} A &= \{A_f\}, \\ B &= \{B_f\}, \\ F &= \{F_f\}. \end{aligned} \tag{4-2}$$

4.3 MODAL TRANSFORMATION

The original system may be described by the vector-matrix equation,

$$[m] \ddot{\underline{x}} + [k] \underline{x} = \underline{F} \tag{4-3}$$

where $[m]$ is the mass matrix; $[k]$ is the stiffness matrix, \underline{F} is the force/torque vector, and \underline{x} is the system state vector.

Equation (4-3) may be transformed into modal coordinates (n) using

$$\underline{x} = Q \underline{n}, \tag{4-4}$$

with Q the modal matrix composed of the normalized eigenvectors.

Substitution of Equation (4-4) into (4-3) yields

$$\underline{k} + [\omega^2] \underline{n} = Q^T \underline{F} = \underline{T}_c. \tag{4-5}$$

The torque, T_c , is of the form

$$T_c = K_p \theta + K_d \dot{\theta}, \tag{4-6}$$

where θ and $\dot{\theta}$ represent angular and angular rate displacements. It is assumed that the rate, $\dot{\theta}$, is measured directly and that

$$\dot{\theta} = \sum \phi_j n_j. \quad (4-7)$$

4.4 GENERAL FORM OF CONTROLLER

The large scale system represented by Equation (4-3) or (4-5) is to be controlled by a conventional rate ($\dot{\theta}$) plus position (θ) controller. Knowledge of the damping ratio ζ_j and frequency ω_j of each of the modes is assumed. The general form of the PD controller used is shown in Figure 4-1.

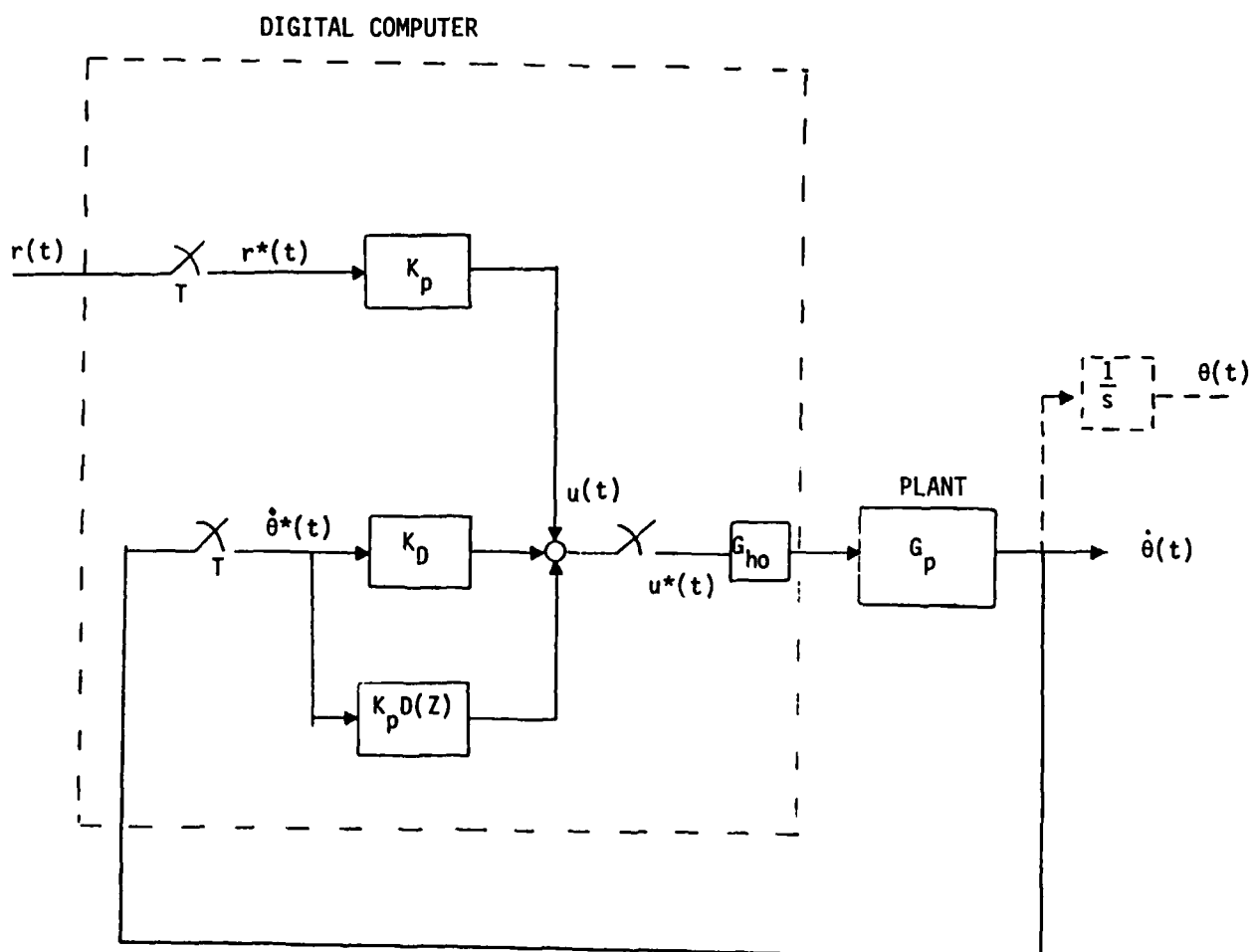


FIGURE 4-1. PROPORTIONAL (θ) - DERIVATIVE ($\dot{\theta}$) CONTROL LAWS

4.5 PLANT DESCRIPTION

Each path shows the transfer function, η_j/T_c , and the overall transfer function of the plant, $\dot{\theta}/T_c$, is given by:

$$\frac{\dot{\theta}(s)}{T_c(s)} = \sum_{j=1}^N \phi_j \frac{\eta_j(s)}{T_c(s)} \quad (4-8)$$

This plant is portrayed graphically in Figure 4-2.

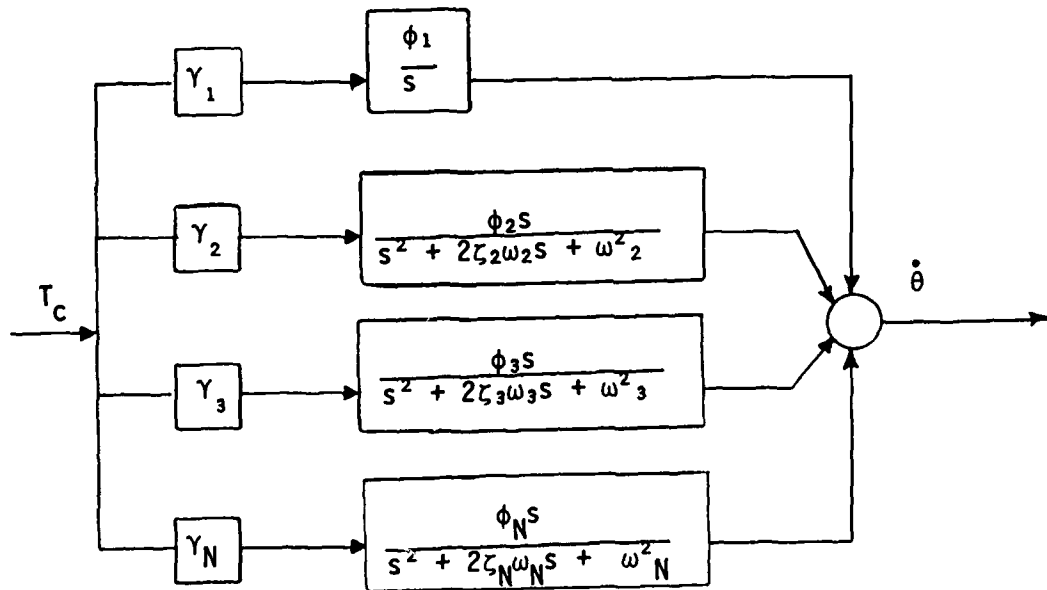


FIGURE 4-2. PLANT DESCRIPTION

4.6 DERIVATION OF THE CHARACTERISTIC EQUATION

Using standard feedback control simplifying techniques, one can show that the transfer function corresponding to the control system shown in Figure 4-1, is given by

$$\frac{\dot{\theta}^*}{r^*} = \frac{K_p G_p^*}{1 + [K_d + K_p D_f(z)] G_p^*} \quad (4-9)$$

where

$$G_p(s) = \sum_{i=1}^N \phi_i \gamma_i P_i(s), \quad (4-10)$$

$$G_p^*(z) = Z[G_{ho}(s) G_p(s)] \quad (4-11)$$

$$P_i(s) = \frac{s}{s^2 + 2\zeta_i \omega_i s + \omega_i^2} \quad (4-12)$$

$$D_f(z) = \frac{T(z+1)}{2(z-1)}, \quad (4-13)$$

$$G_{ho}(s) = \frac{1 - e^{-Ts}}{s} \quad (4-14)$$

with γ_i , ϕ_i denoting the slope of the i th mode at torquer, sensor (respectively), and ζ_i , ω_i denoting the damping ratio, natural frequency of the i th mode. The sample time is T .

Notation: The following, frequently appearing quantities in the derivation are represented by the given symbol:

$$\alpha_1 \equiv \zeta_1 \omega_1$$

$$\beta_1 \equiv \omega_1 [1 - \zeta_1^2]^{1/2}$$

$$c_1 \equiv \cos \beta_1 T \quad (4-15)$$

$$s_1 \equiv \sin \beta_1 T$$

$$e_1 \equiv e^{\alpha_1 T}$$

Before deriving the characteristic equation, three lemmas will be stated which simplify the derivation.⁴

Lemma 1.

$$\begin{aligned} Z[G_{h_0}(s) G(s)] &= Z[(1 - e^{-Ts}) G(s)/s] \\ &= (1 - z^{-1}) \cdot Z[G(s)/s] \end{aligned} \quad (4-16)$$

Lemma 2.

$$Z\left[\frac{b}{(s+a)^2 + b^2}\right] = \frac{z e^{-aT} \sin bT}{z^2 - 2ze^{-aT} \cos bT + e^{-2aT}} \quad (4-17)$$

Lemma 3. If $\omega \neq 0$, then

$$Z\left[\frac{1}{s^2 + 2\zeta\omega s + \omega^2}\right] = \frac{1}{\omega(1 - \zeta^2)^{1/2}} \quad (4-18)$$

$$\cdot \frac{z e^{-\zeta\omega T} \sin[\omega(1-\zeta^2)^{1/2}T]}{z^2 - 2ze^{-\zeta\omega T} \cos[\omega(1-\zeta^2)^{1/2}T] + e^{-2\zeta\omega}}$$

Proof:

(First complete the square of the denominator, then combine the linearity of the Z transform with Lemma 2 to obtain the stated result).

Restating Lemma 3 using the notation in Equations (4-15) yields

$$Z\left[\frac{1}{s^2 + 2\zeta\omega s + \omega^2}\right] = \frac{1}{\beta} \cdot \frac{esz}{z^2 - 2ecz + e^2} \quad (4-19)$$

Finally, if $\omega = 0$, then

Lemma 4.

$$Z\left[\frac{1}{s^2}\right] = \frac{Tz}{(z-1)^2} \quad (4-20)$$

Note: Lemma 4 can be shown to be the limiting case of Lemma 3 as $\omega \rightarrow 0$ using L'Hospital's Rule.

With the aid of the above limits, the characteristic equation can now be derived. Equation (4-13) will replace $D_f(z)$, but the expression for $G_p^*(z)$ will have to be found.

$$\begin{aligned}
 G_p^*(z) &= z[G_{ho}(s) G_p(s)] \\
 &= (1-z^{-1}) z[G_p(s)/s] , \text{ by Lemma 1} \quad (4-21)
 \end{aligned}$$

$$\begin{aligned}
 &= (1-z^{-1}) \sum_{i=1}^N \phi_i \gamma_i z[1/(s^2 + 2\zeta_i \omega_i s + \omega_i^2)] \\
 &= \frac{z-1}{z} \left[\phi_1 \gamma_1 \cdot \frac{Tz}{(z-1)^2} + \sum_{i=2}^N \frac{\phi_i \gamma_i}{\beta_i} \cdot \frac{e_i c_i z}{z^2 - 2e_i c_i z + e_i^2} \right]
 \end{aligned}$$

using Lemma 4 and 3.

Next, substitute $D(z)$, $G_p^*(z)$ into the denominator of the transfer function θ^*/r^* , i.e., Equation (4-9), to obtain the characteristic equation.

$$\begin{aligned}
 &1 + [K_d + K_p \cdot \frac{T}{2} \cdot \frac{z+1}{z-1}] \cdot \frac{z-1}{z} \cdot [\phi_1 \gamma_1 \frac{Tz}{(z-1)^2} \\
 &+ \sum_{i=2}^N \frac{\phi_i \gamma_i}{\beta_i} \cdot \frac{e_i c_i z}{z^2 - 2e_i c_i z + e_i^2}] = 0 . \quad (4-22)
 \end{aligned}$$

Cancelling and multiplying by $z-1$ yields

$$\begin{aligned}
 &1 + [K_d(z-1) + K_p \frac{T}{2} (z+1)] \cdot [\frac{\phi_1 \gamma_1 T}{(z-1)^2} \\
 &+ \sum_{i=2}^N \frac{\phi_i \gamma_i}{\beta_i} \frac{e_i s_i}{z^2 - 2e_i c_i z + e_i^2}] = 0 .
 \end{aligned}$$

Finally, we obtain the C.E. in polynomial form by combining the finite sum inside brackets into a single fraction and multiplying through by the denominator. Let

$$H_i = \frac{\phi_1 Y_1 e_i c_i}{B_i}, \quad i=2, 3, \dots, N, \quad (4-24)$$

then

$$\frac{N^*}{D^*} = \frac{\phi_1 Y_1 T}{(z-1)^2} + \sum_{i=2}^N H_i \cdot \frac{1}{z^2 - 2e_i c_i z + e_i^2} \quad (4-25)$$

Combining yields

$$\begin{aligned} \frac{N^*}{D^*} &= [\phi_1 Y_1 T \cdot \prod_{i=2}^N (z^2 - 2e_i c_i z + e_i^2) \\ &\quad + \sum_{k=2}^N H_k (z-1)^2 \cdot \prod_{\substack{i=2 \\ i \neq k}}^N (z^2 - 2e_i c_i z + e_i^2)] / D^* \end{aligned} \quad (4-26)$$

where

$$D^* = (z-1)^2 \prod_{i=2}^N (z^2 - 2e_i c_i z + e_i^2) \quad (4-27)$$

Substituting and multiplying through by D^* gives the C.E. in polynomial form (albeit not the most convenient form):

$$D^* + [K_d(z-1) + K_p \cdot \frac{T}{2}(z+1)]N^* = 0. \quad (4-28)$$

or

$$(z-1)^2 \prod_{i=2}^N (z^2 - 2e_i c_i z + e_i^2) + [K_d(z-1) + K_p \frac{T}{2}(z+1)] .$$

$$[\phi_1 Y_1 T \prod_{i=2}^N (z^2 - 2e_i c_i z + e_i^2)] \quad (4-29)$$

$$+ \sum_{k=2}^N \frac{\phi_k Y_k e_k s_k}{\beta_k} (z-1)^2 \prod_{i=2, i \neq k}^N (z^2 - 2e_i c_i z + e_i^2) = 0.$$

4.7 ALGORITHMIC DEVELOPMENT OF PARAMETER PLANE FORM OF C.E.

For the parameter plane analysis, let k_0, k_1 be the two parameter of interest. Then, the characteristic equation must be in the form

$$C.E. = \sum_{i=0}^M (A_i k_0 + B_i k_1 + F_i) z^i . \quad (4-1)$$

For this application,

$$k_0 = K_d, \quad k_1 = K_p + T/2. \quad (4-30)$$

The objective then will be to develop an algorithmic approach that will transform the characteristic equation given in Equation (4-15) into the form of Equation (4-1), that is, generate the arrays A, B, and F.

The following algorithm for multiplying polynomials will be instrumental in achieving the above goal. As can be seen from Equation (4-29), the polynomial product

$$P_{2N}(z) = \prod_{f=1}^N (z^2 + a_f z + b_f) \quad (4-31)$$

occurs quite frequently. Suppose that the resulting polynomial is of degree m . Let $p_{m,j}$ denote the coefficient of the z^j term in this polynomial. For example, if $N=1$, then

$$P_2(z) = p_{2,2}z^2 + p_{2,1}z + p_{2,0} \quad (4-32)$$

where

$$p_{2,2} = 1, \quad p_{2,1} = a_1, \quad p_{2,0} = b_1 \quad . \quad (4-33)$$

ALGORITHM P: Let $N \geq 2$ be specified. Then the coefficients of the polynomial,

$$P_{2N}(z) = \prod_{i=1}^N (z^2 + a_i z + b_i)$$

can be determined recursively by

$$p_{2m,0} = p_{2m-2,0} b_m$$

$$p_{2m,1} = p_{2m-2,1} b_m + p_{2m-2,0} a_m$$

$$p_{2m,i} = p_{2m-2,i} b_m + p_{2m-2,i-1} a_m + p_{2m-2,i-2}$$

for $i = 2, 3, \dots, 2m - 2$.

$$p_{2m,2m-1} = p_{2m-2,2m-2} a_m + p_{2m-2,2m-3}$$

$$p_{2m,2m} = p_{2m-2,2m-2} \quad (4-34)$$

where $m = 2, 3, \dots N$

Notes: 1. All intermediate products are available as well as the final polynomial - the order of calculation is

$P_2(z)$ given, the $P_4(z), P_6(z), \dots, P_{2N}(z)$.

2. Although it is possible to derive closed form expressions for the coefficients of $P_{2N}(z)$, the above recursive approach is more accurate computationally.

Proof:

The proof is a standard application of the method of mathematical induction.

The desired form of the characteristic equation, Equation (4-1), can now be obtained from Equation (4-29). The goal will be to generate polynomials $D(z)$ and $H(z)$ so that the characteristic polynomial can be expressed as

$$D(z) + [K_d(z-1) + K_p \frac{T}{2}(z+1)] H(z). \quad (4-35)$$

The general procedure is outlined in Figure 4-3. Note that $D(z)$ and $H(z)$ have degree $2N$ and $2N-2$, respectively.

Each step in the procedure is discussed with computational efficiency in mind.

Step 1. The polynomial

$$D(z) = D_{2N}(z) \quad (4-36)$$

can be obtained using ALGORITHM P with initial values of

$$d_2 = 1, \quad d_1 = -2, \quad d_0 = 1. \quad (4-37)$$

Notation: Let c_i denote the coefficient of z^i in polynomial $C(z)$, i.e. for $D(z)$ of degree $2N$, obtained in Step 1,

$$D(z) = d_{2N} z^{2N} + d_{2N-1} z^{2N-1} + \dots + d_2 z^2 + d_1 z + d_0 \quad (4-38)$$

Step 2. Obtain the coefficients of $G(z)$ from those of the previously calculated $D(z)$. Since

$$D(z) = (z^2 - 2z + 1) \cdot G(z), \quad (4-39)$$

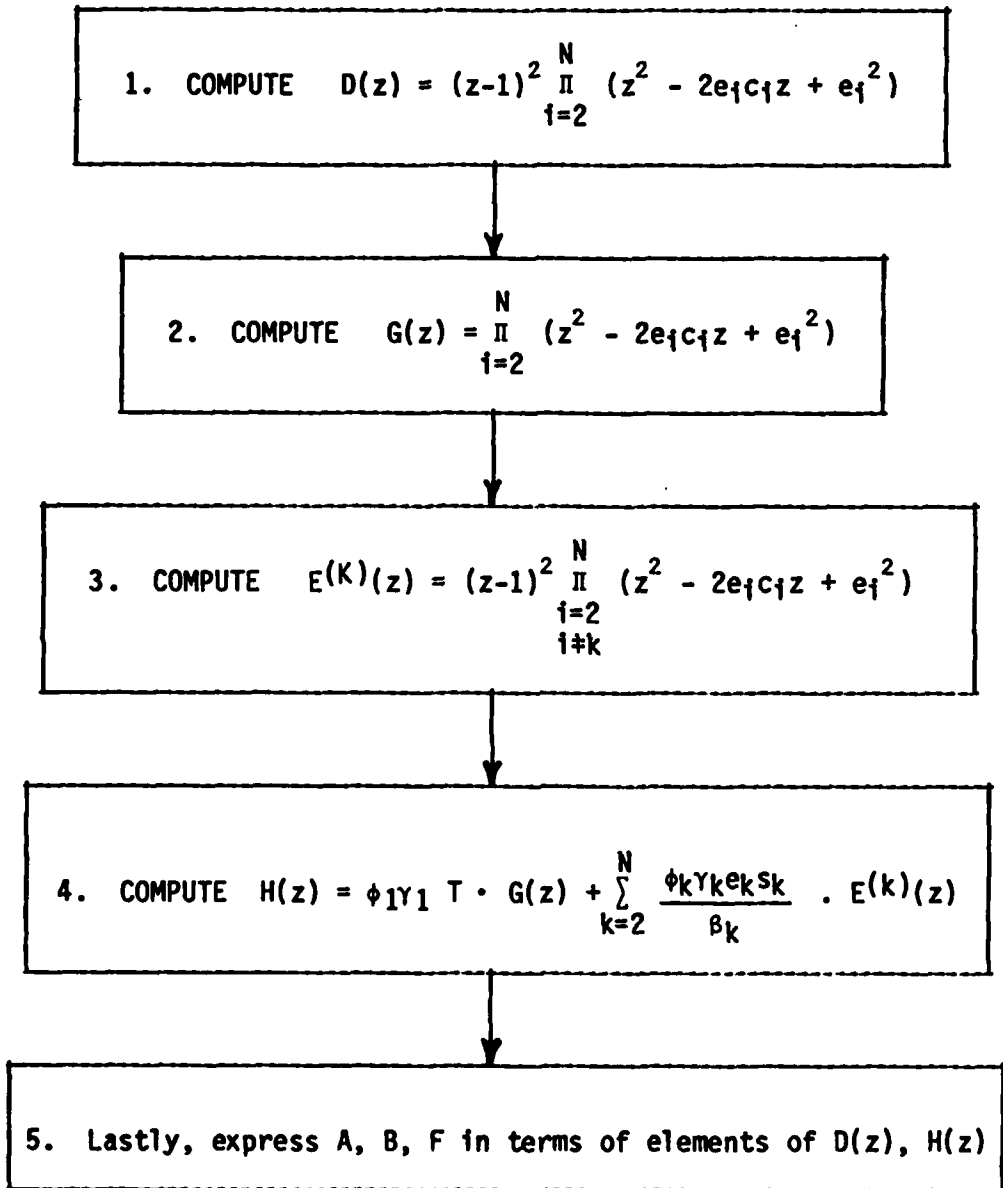


FIGURE 4-3. PROCEDURE FOR OBTAINING ARRAYS A, B, AND F.

multiply out the right-hand side, equate coefficients, and solve for the coefficients g_i , $i=0, 1, 2, \dots, 2N-2$ to obtain

$$g_{2N-2} = d_{2N}$$

$$g_{2N-3} = d_{2N-1} + 2g_{2N-2} \quad (4-40)$$

$$g_{2N-2-i} = d_{2N-i} + 2g_{2N-1-i} - g_{2N-i}$$

for $i = 2, 3, \dots, 2N-2$.

Step 3. Express the coefficients of $E^{(K)}(z)$ in terms of those of $D(z)$, K given.
To do this, let

$$\begin{aligned} D(z) &= (z-1)^2 \prod_{i=2}^N (z^2 + a_i z + b_i) \\ &= (z^2 + a_k z + b_k) \left[(z-1)^2 \prod_{\substack{i=2 \\ i \neq k}}^N (z^2 + a_i z + b_i) \right] \\ &= (z^2 + a_k z + b_k) \cdot E^{(k)}(z) \end{aligned} \quad (4-41)$$

where (referring to Equation (4-15)),

$$a_i = -2e_i c_i, \quad b_i = e_i^2 \quad (4-42)$$

As done above in Step 2, multiply out Equation (4-42), equate coefficients, and solve for coefficient $e_i^{(K)}(z)$, $i=0, 1, 2, \dots, 2N-2$ to obtain

$$e^{(K)}_{2N-2} = d_{2N}$$

$$e^{(K)}_{2N-3} = d_{2N-1} - a_k e^{(K)}_{2N-2} \quad (4-43)$$

$$e^{(K)}_{2N-2-i} = d_{2N-i} - b_k e^{(K)}_{2N-i} - a_k e^{(K)}_{2N-1-i}$$

for $i=2, 3, \dots, 2N-2$.

STEP 4. Adding corresponding terms yields for $H(z)$,

$$h_i = \phi_1 Y_1 T g_i + \sum_{k=2}^N \frac{\phi_k Y_k e_k s_k}{\beta_k} e^{(k)}_i \quad (4-44)$$

for $i=2N-2, 2N-3, \dots, 2, 1, 0$.

Step 5. With $H(z)$ and $D(z)$ obtained, the characteristic polynomial becomes

$$D(z) + [K_d (z-1) + K_p \frac{T}{2} (z+1)] \cdot H(z) . \quad (4-45)$$

With k_0, k_1 being the two parameters of interest as given in Equation (4-30), the arrays A, B, and F can be obtained. For example, the coefficient of z^2 is given by

$$d_2 + K_d \cdot h_1 + K_p \cdot \frac{T}{2} h_1 - h_2 \cdot K_d + K_p \frac{T}{2} h_2 . \quad (4-46)$$

Collecting the appropriate terms as shown in Equation (4-1) yields

$$A_2 = h_1 - h_2, B_2 = h_1 + h_2, F_2 = d_2 \quad (4-47)$$

The complete arrays are given in the following Table 4.1.

z^i	A_i	B_i	F_i
z^{2N}	0	0	d_{2N}
z^{2N-1}	h_{2N-2}	h_{2N-2}	d_{2N-1}
z^{2N-2}	$h_{2N-3} - h_{2N-2}$	$h_{2N-3} + h_{2N-2}$	d_{2N-2}
z^{2N-3}	$h_{2N-4} - h_{2N-3}$	$h_{2N-4} + h_{2N-3}$	d_{2N-3}
.	.	.	.
.	.	.	.
.	.	.	.
z^2	$h_1 - h_2$	$h_1 + h_2$	d_2
z^1	$h_0 - h_1$	$h_0 + h_1$	d_1
z^0	$-h_0$	$+h_0$	d_0

TABLE 4.1. TWO PARAMETER FORM OF CHARACTERISTIC EQUATION
 (ARRAYS A, B, AND F)

4.8 VERIFICATION

In previous contractual work on large space structures, the parameter space approach was employed with one bending mode. Subsequently, a second bending mode was added. The results obtained with the new algorithm that is designed to handle an arbitrary number of bending modes are in agreement with those of the previous work.

4.9 CONCLUSIONS AND RECOMMENDATIONS FOR FUTURE STUDY

The development of this algorithm removes a serious drawback in the application of the parameter plane approach to the problem of discrete control of large space structures. If the number of desired bending modes exceeds two, then the task of obtaining the necessary form of the characteristic equation becomes extremely complex. Once the modal representation is available, the automation of the generation of the needed arrays A, B, F eliminates this drawback. Previous work by Asner and Seltzer had extended the parameter plane approach to arbitrarily, high order continuous control systems. It is anticipated that this algorithm will now be employed in conjunction with the modal representation of the DARPA flexible large scale space structure developed by Control Dynamics.

Several areas of possible extension of this work follow:

- 1) Include sensor, torquer dynamics
- 2) Allow for more than one sensor, torquer pair.
- 3) Include structural damping at the start, rather than introducing it later into the modal representation.
- 4) Introduce a second integrator into the feedback loop with a corresponding control gain. Preliminary work indicates that the same line of development can be used and that the needed arrays A, B, C, F can be generated by the computer.

REFERENCES

1. Siljak, D. D., Nonlinear Systems, Wiley, New York, 1969.
2. Seltzer, S. M., "Sampled-Data Control System Design in the Parameter Plane", Proc. of Eighth Annual Allerton Conferences on Circuit and System Theory, Monticello, ILL., 1970, pp. 454-463.
3. Asner, B. A. and Seltzer, S. M., "Parameter Plane Analysis for Large Flexible Spacecraft", Journal of Guidance and Control, Vol. 4, No. 3, May-June, 1981, pp. 284-290.
4. Kuo, C. K., Digital Control Systems, SRL Publishing, ILL., 1977.

5.0 CONCLUSIONS

With the exception of Task 1 (Investigation of Structural Damping Models), all remaining six tasks were completed on time and within schedule. The development and prescription of an orderly approach to the implementation of the developed digital control analysis techniques was performed under Task 2 and reported upon in Section 3.0. Closely associated with the work under Task 2 was the extension (to the digital domain) of the decomposition principal (Parameter Space). This was reported upon in Section 4.0. All modeling tasks (Tasks 3, 5-76) are reported upon in Section 2.0. The unique analysis technique, embodying a combination of finite element modeling, closed-form solutions of continuous beams, and modal synthesis, is reported upon in Section 2.0. This work (Tasks 3, 5-7) presents a means of better understanding the actual dynamics of the resulting mathematical model.

APPENDIX A TO FINAL TECHNICAL REPORT FOR
ACOSS FIFTEEN
(ACTIVE CONTROL OF SPACE STRUCTURES)

DARPA - WPAFB

VCOSS DYNAMIC MODEL

ABSTRACT

This report presents analysis results of future Large Space Structures (LSS) that can be used by VCOSS Contractors in their control system analyses. The data is presented in the form of modal data for two different "configurations" of a candidate LSS. The analysis technique utilized is a combination of finite element, uniform beam theory and modal synthesis. The model was developed to be not only representative of LSS characteristics but also to be readily amenable to modification and adjustment as required. The model used in this analysis was derived from a model presented in DARPA Report #R-1404 "Active Control of Space Structures Interim Report" by the Charles Stark Draper Laboratory, Inc.

TABLE OF CONTENTS

	<u>Page</u>
ABSTRACT	i
TABLE OF CONTENTS	ii
1.0 INTRODUCTION	1
2.0 LSS QUALITIES/REQUIREMENTS	2
3.0 VCOSS ANALYSIS DESCRIPTION	3
3.1 OPTICAL TRUSS	6
3.2 LIGHT PATH ANALYSIS	9
3.3 EQUIPMENT SECTION	11
3.4 COUPLED ANALYSIS	13
4.0 SUMMARY/CONCLUSIONS	14

1.0 INTRODUCTION

The purpose of this report is to present the results of an analysis activity undertaken to develop detailed structural models of two candidate LSS models labeled Stiffness and Strength. The analysis procedure is presented in an overview format. A later technical report is planned to cover in detail the technical derivation. Results are presented in the form of modal deflections for the optical structure and the equipment section independently, in addition to coupled mode shapes for the complete structure. These uncoupled data are presented in this manner to facilitate analysis by the VCOSS contractors.

2.0 LSS QUALITIES/REQUIREMENTS

What is a Large Space Structure? A question that appears to have an obvious answer -- A large structure in space. However, a more careful examination reveals that the answer is too simple and does not get to the heart of the matter. The space program has spawned a number of "Large Space Structures" in the past if size is the only criteria. The Saturn class of launch vehicles weighed over 5 million pounds, and the Skylab weighed almost two hundred thousand (200,000) pounds. Both programs were very successful in the 1960's and early 1970's. Thus mere physical size is not enough to completely describe LSS even though it must be an ingredient. What then are the appropriate characteristics? It is our opinion that an LSS is characterized as follows:

SUMMATION OF:

- LARGE DIMENSION
- LOW STIFFNESS
- PRECISION POINTING REQUIREMENTS
- HIGH MODAL DENSITY
- LOW FUNDAMENTAL FREQUENCY
- DISTRIBUTED ACTUATORS AND SENSORS

However, to this list a very important ingredient must be added. It is important to realize that we are trying to extend the capability of control systems to as high a degree as possible. Therefore the characteristic that makes an LSS unique is the fact that it includes, in addition to the above,

STATE-OF-THE-ART CONTROL SYSTEM TECHNOLOGY !

It is through this added ingredient that the full dimension of LSS is obtained. It is, therefore, incumbent on the structural analysis to develop a model that not only has large dimension, etc., but also has the ingredients that cause a control system designer difficult. The purpose of this report is to present the results of an analysis activity undertaken to accomplish that task.

3.0 VCOSS ANALYSIS DESCRIPTION

The VCOSS model is derived from a previous model developed for DARPA by the Charles Stark Draper Laboratories (CSDL) and is presented as modeled by Control Dynamics in Figure 1.

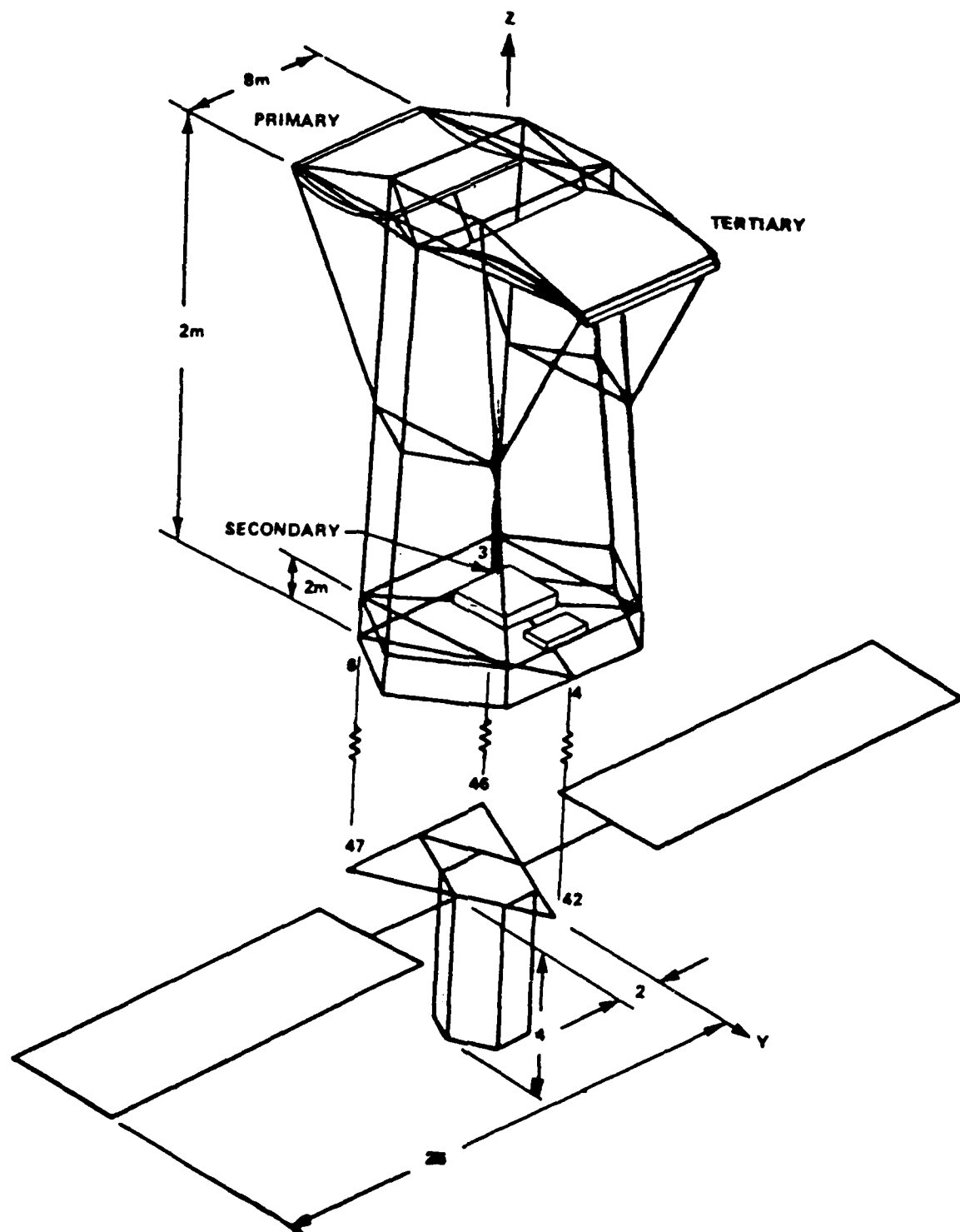


Figure 1

We have undertaken an analysis of this particular structure with the viewpoint of developing a model of a large space structure that would be of sufficient detail and complexity to challenge the capability of control systems designers while retaining management flexibility. The techniques utilized embody a combination of finite element modeling, closed form solution of continuous beams and modal synthesis. Since the light path is of crucial concern in this analysis we have developed an accurate model of the motion of the central ray as a function of the motion of each of the elements in the optical path. In addition, we have constructed our model so that the isolation section stiffness can be readily modified as requirements dictate.

Our analysis procedure will be to employ modal synthesis. This technique has been employed successfully in the past on a number of programs ranging from the Saturn 1 and 1b to the Space Shuttle. It has the distinct advantage in this application in that detail can be applied where necessary and still retain the advantage of being able to make modifications and changes in a minimum of effort. Since the optical truss is the most critical structure, it was modeled in detail as a truss with rigid optical elements. The solar arrays were modeled as continuous uniform beams. The equipment section length was assumed (in that no data was given) and modeled as a uniform beam with equal properties in each direction.

It was required to develop two different models with the same general characteristics in order to illuminate features of the control system design. These two models were termed STRENGTH and STIFFNESS. Their definitions are as follows:

STRENGTH MODEL

The structural characteristics of this model were envisioned to be representative of a class of vehicles that would be designed on the basis of being as light as possible and just being strong enough to withstand the launch environment. Thus the strength model should present low frequency modal data.

STIFFNESS MODEL

The structural characteristics of this model were envisioned to be as stiff as possible. Therefore, high frequencies are to be expected.

It is obvious, certainly, that these two definitions are not only not very precise, but are also rather arbitrary. Therefore, it is very important that the developed structural model not only meet the spirit of these requirements, but

also be readily adaptable to fine tuning and adjustments as required. The Control Dynamics Model meets both of these requirements. The various elements of the Control Dynamics model are contained in the following sections.

3.1 OPTICAL TRUSS

The optical structure is designed to be both stiff and accurate in order to maintain the critical dimensions and spacing of the optical elements. The study model consists of 35 nodes and 117 members. The optical elements contain the most significant mass of the structure and are modeled as rigid bodies suspended on special kinematic mounts attached to the structure in such a way that no structural loads are carried through the mirrors. More will be said on this later.

There are 4 elements in the optical path. These are called the primary, secondary, tertiary and focal plane assembly respectively. Since all the mass is concentrated in the optical elements which are modeled as rigid bodies, this system has 24 degrees of freedom. Since there are 35 nodes for which 105 coordinates are required to specify the configuration, there are 81 coordinates that must be eliminated from the model description. Because of the rigor required in this elimination, it was considered important to include a detailed derivation.

The positions of the nodes are known from the structural definition. The rigid body coordinates can be expressed in terms of the nodal coordinates. To do this we must first look at the supports for the optical elements. They are assumed supported at three points identified as A, B, and C for convenience. The support at point A is considered to have translation stiffness which acts in the three coordinate directions. At point B the support is considered to have stiffness in only two directions and provides no stiffness along the line connecting A and B. At point C the support has stiffness only in the direction normal to the plane containing A, B, and C. Since any or all of the support points can occur at points other than node points of the structure, it may be written as a linear combination of positions of adjacent nodes. The positions of the support points can also be expressed in terms of the rigid body translation and rotation of the optical elements.

The transformation between nodal and rigid body coordinates can be expressed as follows:

$$P \ X = Q \ R, \quad (1)$$

where

P - matrix to combine nodal displacements as required where attach points are located at points other than a node.

X - vector of nodal displacements

Q - matrix relating rigid body motion to nodal displacements

R - vector of rigid body motions of optical elements

Since many of the nodal displacements do not directly figure in the rigid body motion of the optical elements, the size of the structural analysis problem can be significantly reduced by eliminating these coordinates. This is most easily accomplished by first arranging the massless nodes to be the first (or topmost) elements in the nodal position vector for the system. The massless nodes must be at all times in equilibrium so that we can write the force vector in a partitioned form:

$$\begin{bmatrix} K_U & | & K_C \\ \hline K_C^T & | & K_U \end{bmatrix} \begin{bmatrix} X_U \\ \hline X_L \end{bmatrix} = \begin{bmatrix} 0 \\ \hline F_L \end{bmatrix} \quad (2)$$

The vector X_U represents the displacement vector for the massless nodes. In our model 78 nodal displacement components do not directly affect the position of the optical elements. This leaves 27 that do. Since the 4 rigid bodies require only 24 components to completely specify their positions, we can perform a second reduction step by eliminating these. The first reduction step requires calculation of the inverse of the upper part of the structural stiffness matrix K_U . Since this is a 78×78 matrix, this step promises to be an expensive step. This process can be simplified by taking advantage of the symmetry and sparseness of the matrix K_U . Since K_U is part of a structural stiffness matrix it is non-negative definite. This means that the diagonal elements are nonnegative and are in fact zero only if the node is completely decoupled from the rest of the structure in that dimension. That is, if a diagonal element vanishes the whole row and column in which it lies will also vanish. It is relatively easy to construct a lower triangular matrix Q which converts K_U into a lower triangular matrix such that $Q K_U Q^T$ is the identity matrix. If we define a new vector X'_U such that

$$X_U = Q^T X'_U \quad (3)$$

We can solve for X'_U and eliminate it from the force equation and determine an effective stiffness matrix.

$$K_E = K_l - K_l^T Q^T Q K_l \quad (4)$$

With this effective stiffness matrix we now wish to reduce the size of our system

to the minimum and convert from nodal displacements to rigid body motions involving translations and rotations of optical elements. The reduction process is similar to the above in that we select a subset of the 27 coordinates to eliminate and call them X_U . We must solve for the X_U in terms of the remaining coordinates and substitute for them in the equations (1) and (2) to arrive at a transformation expressing the remaining nodal variables in terms of rigid body coordinates. This transformation must then be applied to the reduced, effective stiffness matrix. The mathematics involved in this process is straightforward, although tedious, and will not be presented in detail in this report. The results of this last step, though, is to produce an effective stiffness matrix in terms of rigid body motions of the four optical elements and the stiffness properties of the truss structure.

Before presenting results for the optical structure, one further observation must be made. It is noted that the focal plane is mounted in such a manner as to allow essentially free motion along the line of sight of the optical truss. This is considered an unsatisfactory design feature and therefore was selected as a candidate for added stiffness for the stiffness model. We, therefore, selected to differentiate between our Stiffness model and our Strength model by the stiffness of this section. The truss itself is efficiently designed to carry the loads and no appreciable weight savings are expected to accrue through reductions in the truss elements. The modal data for the optical truss section is presented in Table 1 for the Stiffness model and in Table 2 for the Strength model.

3.2 LIGHT PATH ANALYSIS

The light path analysis was accomplished by considering the mirrors as thin spherical mirrors with all centers of curvature on the optical axis. The light ray configuration is given in Figure 2 and is based on the referenced CSDL report.

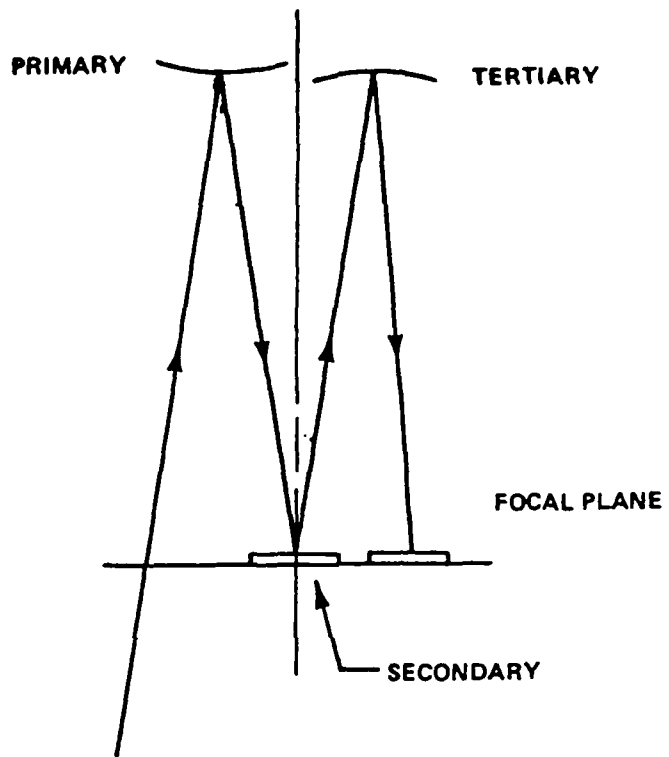
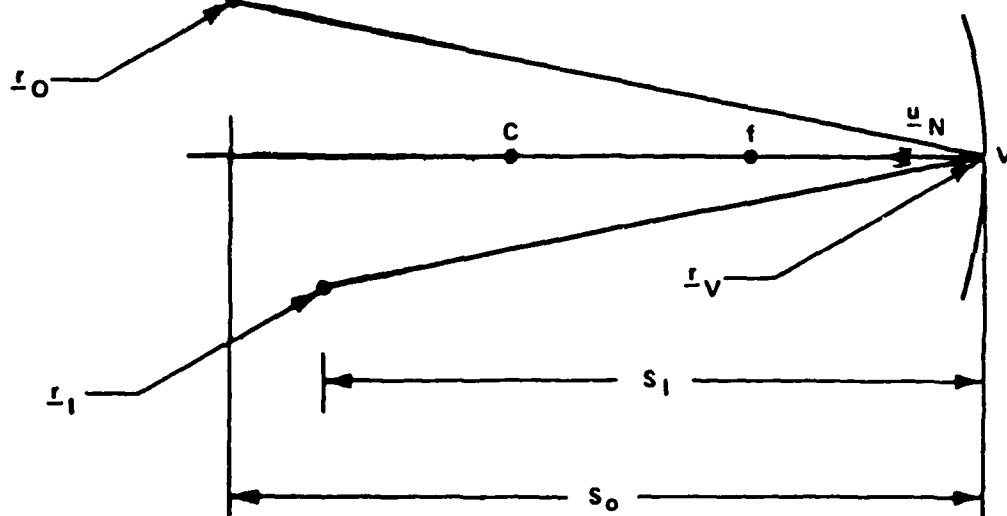


Figure 2

The geometry considerations utilized in determining the effects of flexibility motion and rigid body motion at each of the optical elements on the light path is given in Figure 3. We analyzed each mirror under the assumptions as given and as illustrated in the Figure. The vector equation was processed for each mirror taking the object of each mirror as the image of the preceeding mirror in the chain (except for the first mirror where the object was assumed to be at infinity). The result of this analysis was programmed so that we could easily develop the effect of each mode shape on the light path error (or apparent error). The result is that for each mode shape there are three values (x , y , z translation at the focal plan) that represent the contribution of that particular mode to the error in location of the image. These three error numbers are presented with each mode in the appropriate section of this report.

LIGHT PATH ANALYSIS

$$\frac{1}{s_o} + \frac{1}{s_i} = \frac{2}{R} = \frac{1}{f}$$



$$s_i = r_v + \frac{f}{u_n(r_o - r_v) - f} [2u_n u_n \cdot (r_o - r_v) - (r_o - r_v)]$$

Figure 3

3.3 EQUIPMENT SECTION

The equipment section is composed of solar arrays and equipment module as given in Figure 4.

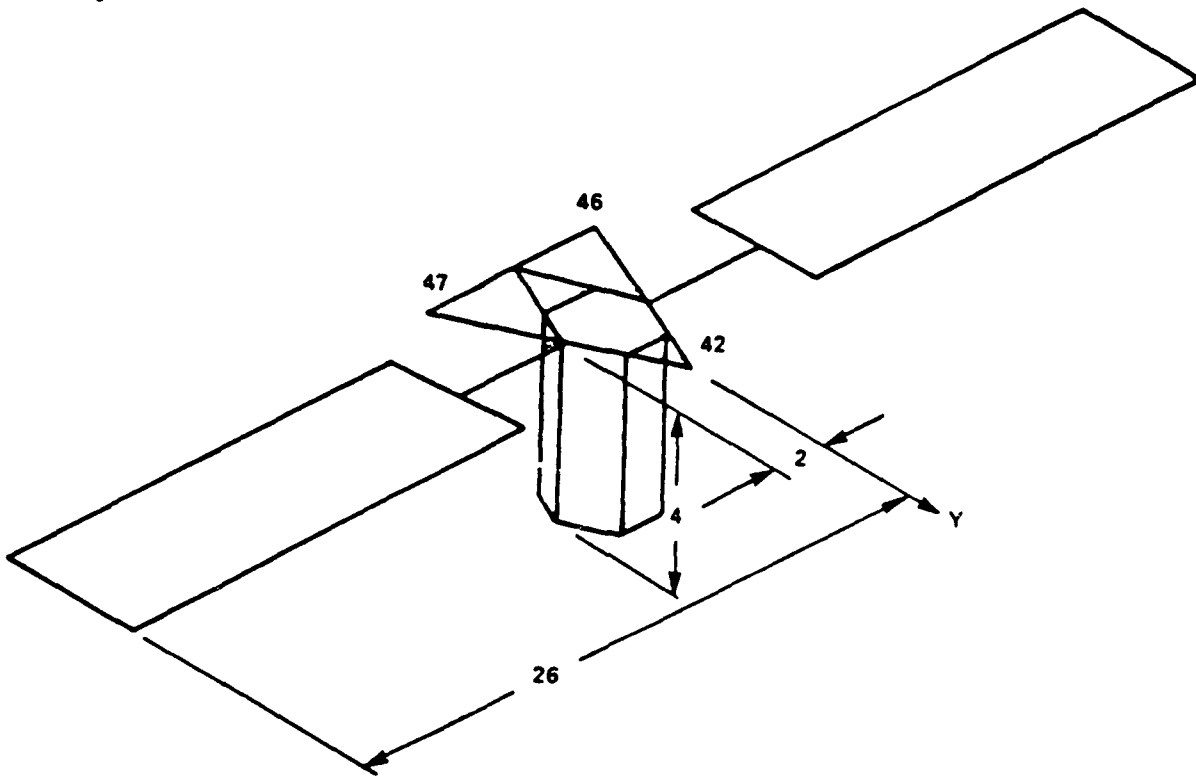


Figure 4

The solar arrays are treated as uniform beams commencing at 2 meters from the centerline and extending to 26 m on either side in the \pm X directions. The mass of each array is 360 kg. The material and section properties are as stated in the DARPA reports with $E = 1.24 \times 10^{11} \text{ N/M}^2$, $A = 9.407 \times 10^{-4} \text{ M}^2$, $I = 1.874 \times 10^{-5} \text{ M}^4$. The central module of the equipment section is modeled as a uniform beam extending 4m along the negative Z direction starting at the origin of coordinates as shown in Figure 4. It has a mass of 3500 kg. The rigid body properties of the equipment section are a mass of 4220 kg and moments of inertial of $I_{xx} = 5890 \text{ kg m}^2$, $I_{yy} = 188069$, $I_{zz} = 185680$. The three uniform beams are combined through the process of modal synthesis to form the equipment section model. This results in mass and stiffness matrices as shown below

$$M_E = \begin{bmatrix} M & 0 & (\int \underline{\Phi} dm) \\ 0 & I & (\int \underline{\Phi} \times \underline{\Phi} dm) \\ (\int \underline{\Phi} dm)^T & (\int \underline{\Phi} \times \underline{\Phi} dm)^T & 1 \end{bmatrix}$$

$$K_E = \begin{bmatrix} 0 & 0 & 0 \\ 0 & 0 & 0 \\ 0 & 0 & \omega_1^2 \quad \omega_2^2 \dots 0 \end{bmatrix}$$

The nodes that make up the input to the model are developed as so-called cantilever modes having one end clamped and one end free. Notice that all coupling is through the mass matrix. Each of the three cantilever beams of the model is truncated after the first 2 bending modes in each of the two transverse axes. Thus the equipment section model has a total of 18 degrees of freedom. The material properties of the center module are $EI = 1.788 \text{ KI}^2 \text{ N/M}^2$ which yields a first bending frequency of .5 Hz. The solar array first bending frequency is .38 Hz. This model as defined constitutes our Strength Model. To generate the Stiffness Model the structures are stiffened by a factor of 10 without changing the mass. The modes of the equipment section are shown in Tables 3 and 4.

3.4 COUPLED ANALYSIS

The development of the coupled model at this point involves the generation of coupled mass and stiffness matrices from the developed components. The stiffness matrix takes the form as given below:

COMBINED SYSTEM STIFFNESS:

$$K = \begin{bmatrix} 0 & 0 & 0 \\ 0 & \omega_{oi}^2 & 0 \\ 0 & 0 & 0 \end{bmatrix} + \sum_i K_i \begin{bmatrix} \Phi_{oi} \\ -\Phi_{ei} \end{bmatrix} [\Phi_{oi}^T; \Phi_{ei}^T]$$

where

ω_{oi}^2 - eigenvalues (natural frequency) of the optical truss

ω_{ei}^2 - eigenvalues of the equipment section

Φ_{oi} - eigenvector of the optical truss

Φ_{ei} - eigenvector of the equipment section

It is noticed that the effect of stiffness changes in the equipment section readily implemented in that one would only have to change the value of the eigenvalues, since the eigenvector is not changed. In addition, the coupling between the equipment section and the optical truss is apparent in the coupling terms in the stiffness matrix. Since the modal synthesis in this case is acting on uncoupled free-free modes, there is no coupling in the mass matrix.

We therefore have all the information that is required to develop the detailed coupled model. We have supplied the intermediate steps to facilitate others who might like to couple these two sections together differently. The coupling was formed using the form of the isolator section as given in the referenced model by CSDL. That is, the isolator springs were considered to be attached at three points on the equipment section and the optical structure.

The result of this coupling operation is presented as modal data in Figures 5 and 6. The modal data is presented in Table 5 for the Stiffness model and in Table 6 for the Strength model.

4.0 SUMMARY/CONCLUSIONS

We have presented a detailed structural model of two forms of future LSS. The form of development of both of these structures enables rapid and efficient alterations of these models in the future if conditions and requirements warrant. It is thought prudent at this point to present these models for review and comment by the VCOSS contractors and others. The data can be quickly changed to emphasize characteristics of LSS that are not sufficiently covered in these current models.

TABLE 1

STIFFNESS MODEL BENDING MODES OF OPTICAL STRUCTURE

(zero frequency modes omitted).

All displacements are in meters.

Modes are normalized to unity generalized mass.

The following table displays modal displacements. The format is as shown.

	JOINT 4	JOINT 3	JOINT 6	LOS ERROR
MODE = N	FREQ =	X.XXXX HZ		
X Translation	X.XXXXXX	X.XXXXXX	X.XXXXXX	X.XXXXXX
Y Translation	X.XXXXXX	X.XXXXXX	X.XXXXXX	X.XXXXXX
Z Translation	X.XXXXXX	X.XXXXXX	X.XXXXXX	X.XXXXXX
MODE = 1	FREQ =	2.2092 HZ		
	-0.005477	0.002359	0.002566	-0.127966
	0.000094	-0.003218	0.003589	-0.005460
	-0.000321	0.015413	-0.016527	-0.004410
MODE = 2	FREQ =	3.5895 HZ		
	-0.025537	0.051599	0.051832	0.073843
	-0.000570	-0.033888	0.033106	0.006635
	0.000023	0.000956	-0.000788	-0.001663
MODE = 3	FREQ =	5.6413 HZ		
	0.001951	-0.005546	-0.003902	-0.004677
	-0.003154	-0.003510	-0.001794	0.190868
	0.005143	0.005797	0.005326	0.009491
MODE = 4	FREQ =	9.7876 HZ		
	0.008534	-0.012636	-0.012658	-0.033210
	0.000664	0.009080	-0.007732	-0.013211
	0.002317	-0.001327	0.002635	0.000962
MODE = 5	FREQ =	10.6198 HZ		
	0.001441	-0.002024	-0.002388	-0.006785
	-0.009365	-0.007086	-0.011950	0.123783
	-0.012824	-0.001294	-0.000018	0.004621

MODE = 6	FREQ =	11.8606	Hz
	-0.021381	0.038098	0.038327
	0.001019	-0.024827	0.027090
	-0.002751	0.007606	-0.008909
			-0.006099
			0.000001
			-0.004296
MODE = 7	FREQ =	18.3524	Hz
	-0.001181	0.005581	0.005063
	-0.000207	-0.002376	0.001783
	-0.004042	-0.001821	0.003761
			-0.011199
			0.015729
			0.004589
MODE = 8	FREQ =	19.0918	Hz
	0.000851	-0.010937	-0.009135
	0.002901	0.006764	-0.000437
	0.019083	0.003554	-0.000746
			0.039565
			0.040702
			-0.025179
MODE = 9	FREQ =	23.7055	Hz
	-0.000240	-0.004564	-0.004179
	0.001101	0.003056	-0.000954
	0.001115	-0.000186	-0.004018
			0.019475
			0.072887
			-0.032830
MODE = 10	FREQ =	24.4272	Hz
	-0.000569	-0.007718	-0.007326
	0.003696	0.006760	0.000474
	0.008617	-0.004658	-0.010399
			0.034363
			0.063281
			-0.039389
MODE = 11	FREQ =	30.5696	Hz
	0.026150	-0.057293	-0.059287
	0.009632	0.051865	-0.034757
	-0.031006	-0.005163	-0.005794
			0.051965
			-0.056568
			0.003104
MODE = 12	FREQ =	32.5465	Hz
	-0.005105	-0.005037	-0.004503
	0.004906	0.004464	0.004884
	0.004028	-0.007363	-0.016295
			0.037886
			-0.297196
			0.035895

MODE = 13	FREQ =	36.0537 HZ	
	-0.004611	0.013281	0.012046
	-0.005616	-0.009569	-0.000164
	0.016966	0.011286	-0.007370
			0.005561
MODE = 14	FREQ =	52.3519 HZ	
	0.042057	0.028234	0.025860
	0.008891	0.017854	-0.001896
	0.029311	-0.095368	0.071788
			0.039530
MODE = 15	FREQ =	66.7940 HZ	
	0.015749	-0.017362	-0.019001
	0.000231	-0.013148	0.016127
	0.038447	0.040765	-0.128205
			0.041543
MODE = 16	FREQ =	71.6937 HZ	
	0.020971	-0.002674	-0.002577
	-0.039879	-0.046937	-0.031331
	-0.019135	0.148159	0.117787
			-0.008513
MODE = 17	FREQ =	83.0792 HZ	
	0.039134	-0.016030	-0.012028
	0.025936	0.034106	0.017050
	0.006834	0.045947	-0.001235
			0.015092
MODE = 18	FREQ =	96.3105 HZ	
	0.036327	0.030580	0.040541
	0.016169	0.007441	0.030574
	-0.062904	-0.074183	-0.064852
			-0.057276

Optical Structure Rigid Body

Properties :

Mass = 5000.0 kg

Center of mass = (0 , 1.5 , 14) m

Inertia Matrix	640500	0	0	
about Mass Center =	0	530000	-10000	kg(m**2)
	0	-10000	210500	

TABLE 2

STRENGTH MODEL BENDING MODES OF OPTICAL STRUCTURE
 (zero frequency modes omitted).
 All displacements are in meters.
 Modes are normalized to unity generalized mass.

The following table displays modal displacements. The format is as shown.

	JOINT 4	JOINT 3	JOINT 6	LOS ERROR
MODE = N	FREQ =	X.XXXXZ		
X Translation	X.XXXXXX	X.XXXXXX	X.XXXXXX	X.XXXXXX
Y Translation	X.XXXXXX	X.XXXXXX	X.XXXXXX	X.XXXXXX
Z Translation	X.XXXXXX	X.XXXXXX	X.XXXXXX	X.XXXXXX
MODE = 1	FREQ =	0.2494HZ		
	0.000003	0.000022	0.000019	-0.000018
	0.001009	0.001008	0.001008	-0.193395
	-0.006684	-0.007402	-0.007391	-0.004965
MODE = 2	FREQ =	2.1996HZ		
	0.005536	-0.001941	-0.002220	0.128133
	0.000102	0.003290	-0.003284	0.002569
	0.000165	-0.015536	0.016395	0.004130
MODE = 3	FREQ =	3.5895HZ		
	-0.025527	0.051836	0.052012	0.073652
	-0.000414	-0.033762	0.033270	-0.000852
	-0.000244	0.000712	-0.001091	-0.001965
MODE = 4	FREQ =	9.7872HZ		
	0.008470	-0.012603	-0.012634	-0.033130
	0.000716	0.009140	-0.007698	-0.014812
	0.002384	-0.001325	0.002630	0.000885

MODE = 5 FREQ = 10.5443HZ
 0.002368 -0.002683 -0.003009 -0.007381
 -0.009401 -0.007190 -0.011705 0.134121
 -0.012620 -0.001341 0.000111 0.005554

MODE = 6 FREQ = 11.8486HZ
 -0.021352 0.038412 0.038439 -0.006034
 0.001101 -0.024471 0.026781 -0.000846
 -0.003063 0.007573 -0.008876 -0.004644

MODE = 7 FREQ = 18.3176HZ
 0.002021 -0.005283 -0.005126 0.017235
 0.002119 0.004958 -0.000702 -0.010512
 0.006853 0.002292 -0.003791 -0.009683

MODE = 8 FREQ = 18.7560HZ
 -0.001950 0.005435 0.005334 -0.035037
 -0.005643 -0.009650 -0.001450 -0.038066
 -0.016733 -0.002980 -0.000298 0.025622

MODE = 9 FREQ = 23.6388HZ
 0.000496 -0.000909 -0.001249 0.018886
 0.003502 0.004307 0.002389 0.072333
 0.001082 -0.001315 -0.005282 -0.036225

MODE = 10 FREQ = 24.3000HZ
 0.000403 -0.001191 -0.001862 0.025116
 0.005935 0.006849 0.004601 0.042542
 0.006996 -0.005202 -0.009588 -0.032689

MODE = 11 FREQ = 28.4961HZ
 -0.010490 0.051218 0.050314 -0.056870
 0.005302 -0.028396 0.039922 -0.067494
 0.011926 -0.003073 0.000668 0.013315

MODE = 12	FREQ =	31.5966HZ	
	0.017613	-0.030292	-0.033559
	0.016836	0.041571	-0.010754
	-0.024793	-0.011680	-0.011282
			0.025628
			-0.245250
			0.027883
MODE = 13	FREQ =	33.6805HZ	
	0.017154	-0.008997	-0.011581
	0.009036	0.020827	-0.004618
	-0.025114	-0.004377	0.014303
			-0.068269
			0.171307
			-0.021296
MODE = 14	FREQ =	52.3323HZ	
	0.041874	0.030036	0.027123
	0.009277	0.018362	-0.001907
	0.029264	-0.094547	0.072900
			-0.635257
			-0.063309
			0.039481
MODE = 15	FREQ =	66.6162HZ	
	0.014681	-0.022448	-0.022308
	0.000134	-0.013301	0.016848
	0.039085	0.030709	-0.134377
			0.590505
			-0.274338
			0.042578
MODE = 16	FREQ =	71.2296HZ	
	0.017704	0.001069	-0.000751
	-0.039503	-0.046675	-0.031931
	-0.015041	0.150875	0.111313
			0.137403
			0.692213
			-0.006537
MODE = 17	FREQ =	78.2946HZ	
	-0.053130	-0.016447	-0.011669
	-0.040125	-0.046498	-0.032059
	0.005073	-0.045349	0.007487
			-0.238157
			-0.111584
			-0.006849
MODE = 18	FREQ =	95.8077HZ	
	0.038259	0.033279	0.042638
	0.015169	0.004422	0.032656
	-0.066658	-0.075998	-0.062458
			-0.027888
			-0.390524
			-0.058708

Optical Structure Rigid Body

Properties :

Mass = 5000.0 kg

Center of mass = (0 , 1.5 , 14) m

Inertia Matrix 640500 0 0
about Mass Center = 0 530000 -10000 kg(m**2)
 0 -10000 210500

TABLE 3

STIFFNESS MODEL BENDING MODES OF EQUIPMENT SECTION

All displacements are in meters.

Modes are normalized to unity generalized mass.

The following table displays modal displacements. The format is as shown.

	JOINT 42	JOINT 46	JOINT 47	ACTUATOR	SENSOR
MODE = N	FREQ =	X.XXXX HZ			
X Translation	X.XXXXXXXX	X.XXXXXXXX	X.XXXXXXXX	X.XXXXXXXX	X.XXXXXXXX
Y Translation	X.XXXXXXXX	X.XXXXXXXX	X.XXXXXXXX	X.XXXXXXXX	X.XXXXXXXX
Z Translation	X.XXXXXXXX	X.XXXXXXXX	X.XXXXXXXX	X.XXXXXXXX	X.XXXXXXXX
			X Rotation	X.XXXXXXXX	X.XXXXXXXX
			Y Rotation	X.XXXXXXXX	X.XXXXXXXX
			Z Rotation	X.XXXXXXXX	X.XXXXXXXX
MODE = 1	FREQ =	0.0000 HZ			
	0.01539373	0.01539373	0.01539373	0.01539373	0.01539373
	0.00000000	0.00000000	0.00000000	0.00000000	0.00000000
	0.00000000	0.00000000	0.00000000	0.00000000	0.00000000
			0.00000000	0.00000000	0.00000000
			0.00000000	0.00000000	0.00000000
			0.00000000	0.00000000	0.00000000
MODE = 2	FREQ =	0.0000 HZ			
	0.00000000	0.00000000	0.00000000	0.00000000	0.00000000
	0.01539373	0.01539373	0.01539373	0.01539373	0.01539373
	0.00000000	0.00000000	0.00000000	0.00000000	0.00000000
			0.00000000	0.00000000	0.00000000
			0.00000000	0.00000000	0.00000000
			0.00000000	0.00000000	0.00000000
MODE = 3	FREQ =	0.0000 HZ			
	-0.00000000	-0.00000000	-0.00000000	-0.00000000	-0.00000000
	-0.00000000	-0.00000000	-0.00000000	-0.00000000	-0.00000000
	0.01539373	0.01539373	0.01539373	0.01539373	0.01539373
			0.00000000	0.00000000	0.00000000
			0.00000000	0.00000000	0.00000000
			0.00000000	0.00000000	0.00000000
MODE = 4	FREQ =	0.0000 HZ			
	0.00000000	0.00000000	0.00000000	0.00000000	0.00000000
	-0.02161667	-0.02161667	-0.02161667	-0.01015032	0.03050308
	0.06514969	-0.06514969	-0.06514969	0.00000000	0.00000000
			0.01302994	0.01302994	
			0.00000000	0.00000000	
			0.00000000	0.00000000	

MODE = 5 FREQ = 0.0000 Hz

 0.00382550 0.00382550 0.00382550 0.00179630 -0.00539812

 -0.00000000 -0.00000000 -0.00000000 -0.00000000 0.00000000

 0.00000000 0.00922362 -0.00922362 -0.00000000 -0.00000000

 0.00000000 0.00000000

 0.00230590 0.00230590

 0.00000000 0.00000000

 MODE = 6 FREQ = 0.0000 Hz

 -0.01160346 0.01160346 0.01160346 0.00000000 -0.00000000

 -0.00000000 -0.00928277 0.00928277 -0.00000000 0.00000000

 0.00000000 -0.00000000 -0.00000000 0.00000000 0.00000000

 0.00000000 0.00000000

 0.00000000 0.00000000

 0.00232069 0.00232069

 MODE = 7 FREQ = 1.2140 Hz

 -0.00000003 -0.00000002 -0.00000002 0.00000042 0.00000745

 0.00000004 0.00000003 0.00000004 0.00000101 -0.00001273

 0.00137836 0.00137849 0.00137859 0.00137845 0.00137845

 -0.00000440 -0.00000935

 0.00000264 0.00000489

 0.00000000 0.00000000

 MODE = 8 FREQ = 1.2238 Hz

 0.00000005 -0.00000008 -0.00000008 0.00000023 -0.00000006

 -0.00112883 -0.00412878 -0.00412888 -0.00261930 0.00160497

 0.00825548 -0.00825549 -0.00825542 0.00000061 0.00000001

 0.00131489 0.00102253

 -0.00000012 0.00000095

 -0.00000001 -0.00000001

 MODE = 9 FREQ = 1.2472 Hz

 0.00096677 0.00096628 0.00096628 0.00032665 -0.00306323

 -0.00000006 0.00000014 -0.00000026 0.00000015 -0.00000240

 0.00000014 0.00232868 -0.00232885 0.00000003 0.00000003

 -0.00000081 -0.00000177

 -0.00001432 -0.00065582

 -0.00000005 -0.00000005

 MODE = 10 FREQ = 1.2477 Hz

 0.00294963 -0.00294970 -0.00294979 0.00000007 0.00000025

 0.00000009 0.00235986 -0.00235988 0.00000008 -0.00000015

 -0.00000018 -0.0000001 0.00000038 0.00000000 0.00000000

 -0.00000003 -0.00000012

 -0.00000004 0.00000047

 -0.00058994 -0.00058994

MODE = 11 FREQ = 1.5817 HZ

 0.00037809 0.00037808 0.00037808 -0.07611863 -0.99964207

 -0.00000262 -0.00000262 -0.00000262 -0.00181729 0.02382944

 0.00003619 -0.00008029 0.00000795 0.00000001 0.00000001

 0.00231204 0.01718096

 -0.35018975 -0.73413873

 -0.00000000 -0.00000000

MODE = 12 FREQ = 1.5821 HZ

 0.00000899 0.00000899 0.00000899 -0.00181123 -0.02378733

 0.00011005 0.00011005 0.00011005 0.07637052 -1.00141907

 -0.00152032 0.00151923 0.00152134 -0.00000002 -0.00000002

 -0.35057145 -0.73462784

 -0.00833309 -0.01746915

 0.00000000 0.00000000

MODE = 13 FREQ = 7.5861 HZ

 0.00000190 -0.00000338 -0.00000338 -0.00000133 0.00000270

 -0.00000022 0.00000189 -0.00000234 -0.00000012 -0.00000059

 0.00071949 0.00071681 0.00072038 0.00071904 0.00071904

 -0.00000027 -0.00000041

 0.00000052 -0.00000381

 -0.00000053 -0.00000053

MODE = 14 FREQ = 7.5875 HZ

 0.00020668 0.00019031 0.00019031 0.00015214 -0.00017924

 0.00000001 0.00000656 -0.00000654 0.00000001 0.00000001

 0.00000261 0.00048152 -0.00047620 0.00000264 0.00000264

 0.00000001 0.00000001

 0.00013729 0.00040573

 -0.00000164 -0.00000164

MODE = 15 FREQ = 7.5876 HZ

 -0.00060411 0.00060946 0.00060946 0.00000201 -0.00000309

 0.00000006 -0.00048537 0.00048549 0.00000009 -0.00000015

 0.00000304 0.00000975 -0.00000316 0.00000317 0.00000317

 0.00000007 -0.00000015

 0.00000161 0.00000500

 0.00012136 0.00012136

MODE = 16 FREQ = 7.6028 HZ

 0.00000002 -0.00000002 -0.00000002 0.00000091 -0.00000295

 0.00217626 0.00217628 0.00217625 0.00206126 -0.00344018

 -0.00435272 0.00435287 0.00435287 0.00000007 0.00000007

 -0.00009290 -0.00294875

 -0.00000143 0.00000251

 -0.00000000 -0.00000000

MODE = 17 FREQ = 9.9097 HZ

-0.00021255	-0.00021255	-0.00021255	0.34756896	-0.99994171
-0.00000012	-0.00000012	-0.00000012	0.00009289	-0.00026724
0.00000018	-0.00001642	0.00001607	0.00000000	0.00000000
			0.00013312	-0.00027221
			-0.49762329	1.01820682
			0.00000000	0.00000000

MODE = 18 FREQ = 9.9102 HZ

-0.00000006	-0.00000006	-0.00000006	0.00009293	-0.00026738
0.00042336	0.00042336	0.00042336	-0.34746578	1.00017655
-0.00063901	0.00063900	0.00063901	0.00000000	0.00000000
			-0.49784425	1.01856959
			-0.00013306	0.00027240
			-0.00000000	-0.00000000

Equipment Section Rigid Body

Properties :

Mass = 4220.0 kg

Center of mass = (0 , 0 , -1.659) m

Inertia Matrix	5890	0	0	
about Mass Center =	0	188069	0	kg(m**2)
	0	0	185620	

TABLE 4

STRENGTH MODEL BENDING MODES OF EQUIPMENT SECTION

All displacements are in meters.

Modes are normalized to unity generalized mass.

The following table displays modal displacements. The format is as shown.

	JOINT 42	JOINT 46	JOINT 47	ACTUATOR	SENSOR
MODE = N	FREQ =	X.XXXX HZ			
X Translation	x.xxxxxxxx	x.xxxxxxxx	x.xxxxxxxx	x.xxxxxxxx	x.xxxxxxxx
Y Translation	x.xxxxxxxx	x.xxxxxxxx	x.xxxxxxxx	x.xxxxxxxx	x.xxxxxxxx
Z Translation	x.xxxxxxxx	x.xxxxxxxx	x.xxxxxxxx	x.xxxxxxxx	x.xxxxxxxx
		X Rotation	x.xxxxxxxx	x.xxxxxxxx	x.xxxxxxxx
		Y Rotation	x.xxxxxxxx	x.xxxxxxxx	x.xxxxxxxx
		Z Rotation	x.xxxxxxxx	x.xxxxxxxx	x.xxxxxxxx
MODE = 1	FREQ =	0.0000 HZ			
	0.01539373	0.01539373	0.01539373	0.01539373	0.01539373
	0.00000000	0.00000000	0.00000000	0.00000000	0.00000000
	0.00000000	0.00000000	0.00000000	0.00000000	0.00000000
			0.00000000	0.00000000	0.00000000
			0.00000000	0.00000000	0.00000000
			0.00000000	0.00000000	0.00000000
MODE = 2	FREQ =	0.0000 HZ			
	0.00000000	0.00000000	0.00000000	0.00000000	0.00000000
	0.01539373	0.01539373	0.01539373	0.01539373	0.01539373
	0.00000000	0.00000000	0.00000000	0.00000000	0.00000000
			0.00000000	0.00000000	0.00000000
			0.00000000	0.00000000	0.00000000
			0.00000000	0.00000000	0.00000000
MODE = 3	FREQ =	0.0000 HZ			
	-0.00000000	-0.00000000	-0.00000000	-0.00000000	-0.00000000
	-0.00000000	-0.00000000	-0.00000000	-0.00000000	-0.00000000
	0.01539373	0.01539373	0.01539373	0.01539373	0.01539373
			0.00000000	0.00000000	0.00000000
			0.00000000	0.00000000	0.00000000
			0.00000000	0.00000000	0.00000000
MODE = 4	FREQ =	0.0000 HZ			
	0.00000000	0.00000000	0.00000000	0.00000000	0.00000000
	-0.02161667	-0.02161667	-0.02161667	-0.01015032	0.03050308
	0.06514969	-0.06514969	-0.06514969	0.00000000	0.00000000
			0.01302994	0.01302994	
			0.00000000	0.00000000	
			0.00000000	0.00000000	

MODE = 5 FREQ = 0.0000 HZ

 0.00382550 0.00382550 0.00382550 0.00179630 -0.00539812

 -0.00000000 -0.00000000 -0.00000000 -0.00000000 0.00000000

 0.00000000 0.00922362 -0.00922362 -0.00000000 -0.00000000

 0.00000000 0.00000000

 0.00230590 0.00230590

 0.00000000 0.00000000

MODE = 6 FREQ = 0.0000 HZ

 -0.01160346 0.01160346 0.01160346 0.00000000 -0.00000000

 -0.00000000 -0.00928277 0.00928277 -0.00000000 0.00000000

 0.00000000 -0.00000000 -0.00000000 0.00000000 0.00000000

 0.00000000 0.00000000

 0.00000000 0.00000000

 0.00232069 0.00232069

MODE = 7 FREQ = 0.3839 HZ

 -0.00000012 0.00000003 0.00000003 0.00000008 0.00000893

 0.00000023 0.00000017 0.00000029 -0.00000037 0.00000584

 0.00137800 0.00137880 0.00137901 0.00137845 0.00137845

 0.00000179 0.00000436

 0.00000328 0.00000412

 0.00000001 0.00000001

MODE = 8 FREQ = 0.3870 HZ

 -0.00000014 0.00000011 0.00000011 0.00000054 0.00000085

 0.00412883 0.00412873 0.00412893 0.00261919 -0.00160293

 -0.00825554 0.00825536 0.00825542 -0.00000008 -0.00000008

 -0.00131405 -0.00102108

 0.00000012 0.00000259

 0.00000002 0.00000002

MODE = 9 FREQ = 0.3944 HZ

 -0.00096867 -0.00096439 -0.00096439 -0.00032582 0.00308009

 -0.00000005 -0.000000176 0.000000166 -0.00000120 0.00001494

 0.00000006 -0.00232895 0.00232858 -0.00000006 -0.00000006

 0.00000514 0.00001098

 0.00002038 0.00066633

 0.00000043 0.00000043

MODE = 10 FREQ = 0.3945 HZ

 -0.00294901 0.00295041 0.00295041 0.00000060 0.00000074

 -0.00000017 -0.00235994 0.00235959 -0.00000044 0.00000456

 0.00000032 0.00000130 -0.00000208 -0.00000003 -0.00000003

 0.00000166 0.00000333

 0.00000092 0.00000226

 0.00058994 0.00058994

MODE = 17 FREQ = 3.1337 HZ

0.00021255	0.00021255	0.00021255	-0.34756863	0.99993885
-0.00000068	-0.00000068	-0.00000068	0.00055795	-0.00160716
0.00000102	0.00001523	-0.00001727	0.00000000	0.00000000
			0.00079876	-0.00163631
			0.49762210	-1.01880670
			0.00000000	0.00000000

MODE = 18 FREQ = 3.1339 HZ

0.00000034	0.00000034	0.00000034	-0.00055803	0.00160501
0.00042336	0.00042336	0.00042336	-0.34746537	1.00017500
-0.00063901	0.00063903	0.00063898	0.00000000	0.00000000
			-0.49784374	1.01856816
			0.00079879	-0.00163589
			0.00000000	0.00000000

Equipment Section Rigid Body

Properties :

Mass = 4220.0 kg

Center of mass = (0 , 0 , -1.659) m

Inertia Matrix 5890 0 0
about Mass Center = 0 188069 0 kg(m**2)
 0 0 185680

TABLE 5

STIFFNESS MODEL BENDING MODES OF COMBINED SYSTEM MODEL
 (zero frequency modes omitted).
 All displacements in meters.
 Modes are normalized to unity generalized mass.

The following table displays modal displacements. The format is as shown

	ACTUATOR	SENSOR	LOS MOTION
MODE = N		FREQ =	X.XXXX HZ
X Translation	x.xxxxxxx	x.xxxxxxx	x.xxxxxxx
Y Translation	x.xxxxxxx	x.xxxxxxx	x.xxxxxxx
Z Translation	x.xxxxxxx	x.xxxxxxx	x.xxxxxxx
X Rotation	x.xxxxxxx	x.xxxxxxx	
Y Rotation	x.xxxxxxx	x.xxxxxxx	
Z Rotation	x.xxxxxxx	x.xxxxxxx	
MODE = 1		FREQ =	0.1772 HZ
	-0.003813	0.002764	-0.000001
	-0.000005	-0.000003	0.000294
	0.000014	0.000014	-0.001087
	-0.000000	0.000002	
	-0.002108	-0.002112	
	0.000074	0.000074	
MODE = 2		FREQ =	0.3552 HZ
	-0.002680	-0.002736	-0.000010
	-0.000003	-0.000009	0.000005
	-0.000021	-0.000071	0.000018
	-0.000002	-0.000002	
	-0.000126	-0.000218	
	0.001623	0.001623	
MODE = 3		FREQ =	0.4040 HZ
	-0.000007	-0.000008	0.000098
	0.001085	0.005469	0.000011
	0.010924	0.010924	-0.000001
	0.001403	0.001226	
	0.000000	-0.000001	
	0.000003	0.000003	
MODE = 4		FREQ =	0.5804 HZ
	-0.000027	-0.000029	-0.005480
	0.007635	0.006916	0.001432
	-0.002575	-0.002575	0.000747
	-0.000221	-0.001100	
	-0.000003	-0.000006	
	-0.000001	-0.000001	

MODE = 5 FREQ = 0.6196 HZ

0.008122	0.009431	-0.001432
0.000021	0.000021	0.001054
-0.000004	-0.000004	0.000000
0.000000	-0.000004	
0.001025	0.001941	
0.000435	0.000435	

MODE = 6 FREQ = 1.1925 HZ

-0.000000	0.000002	0.009431
-0.000898	-0.001116	0.000021
-0.000361	-0.000361	-0.000004
-0.000141	-0.003883	
0.000001	0.000001	
0.000000	0.000000	

MODE = 7 FREQ = 1.2144 HZ

-0.000000	-0.000005	-0.000008
0.000137	-0.000154	-0.124940
-0.001487	-0.001487	-0.001087
-0.000093	-0.000201	
-0.000002	-0.000003	
0.000000	0.000000	

MODE = 8 FREQ = 1.2480 HZ

-0.000418	0.002853	0.000003
0.000000	0.000002	-0.000085
-0.000000	-0.000000	0.000018
0.000001	0.000001	
-0.000050	0.000529	
0.000058	0.000058	

MODE = 9 FREQ = 1.2499 HZ

-0.000140	-0.000007	-0.000271
0.000000	-0.000000	-0.000036
-0.000000	-0.000000	-0.000001
0.000000	0.000000	
-0.000082	-0.000107	
-0.000620	-0.000620	

MODE = 10	FREQ =	1.4901 HZ	
	-0.000001	-0.000008	-0.005480
	0.000294	-0.124940	0.001432
	-0.001087	-0.001087	0.000747
	-0.011142	-0.099322	
	-0.000003	-0.000007	
	-0.000000	-0.000000	
MODE = 11	FREQ =	1.5817 HZ	
	-0.076121	-0.999901	-0.000190
	-0.000274	0.003533	-0.000297
	-0.000001	-0.000001	-0.000525
	0.001239	0.002587	
	-0.350286	-0.734339	
	0.000001	0.000001	
MODE = 12	FREQ =	1.5846 HZ	
	-0.000270	-0.003552	0.000000
	0.077243	-0.994330	0.000000
	0.000172	0.000172	0.000000
	-0.348482	-0.728201	
	-0.001245	-0.002609	
	0.000000	0.000000	
MODE = 13	FREQ =	2.2282 HZ	
	-0.000015	-0.000056	0.009431
	0.000029	-0.000182	0.000021
	0.000012	0.000012	-0.000004
	-0.000069	-0.000111	
	-0.000063	-0.000110	
	-0.000012	-0.000012	
MODE = 14	FREQ =	3.7563 HZ	
	0.000184	-0.000245	0.000001
	-0.000007	0.000006	0.000529
	0.000001	0.000001	0.000058
	0.000003	0.000005	
	-0.000144	-0.000250	
	0.000055	0.000055	

MODE = 15	FREQ =	5.6435 HZ	
	-0.000010	0.000003	0.000000
	0.000005	-0.000085	0.000000
	0.000018	0.000018	0.000000
	-0.000027	-0.000046	
	0.000004	-0.000001	
	-0.000001	-0.000001	
MODE = 16	FREQ =	7.5861 HZ	
	-0.000001	0.000001	0.000003
	-0.000002	-0.000003	-0.000085
	0.000720	0.000720	0.000018
	-0.000001	-0.000001	
	-0.000000	-0.000004	
	-0.000001	-0.000001	
MODE = 17	FREQ =	7.5875 HZ	
	0.000152	-0.000180	-0.000001
	-0.000000	0.000001	0.000019
	0.000003	0.000003	0.000121
	-0.000000	0.000001	
	0.000137	0.000405	
	-0.000006	-0.000006	
MODE = 18	FREQ =	7.5877 HZ	
	0.000008	-0.000014	0.000000
	0.000000	-0.000001	0.000000
	0.000004	0.000004	0.000000
	0.000002	-0.000001	
	0.000005	0.000019	
	0.000121	0.000121	
MODE = 19	FREQ =	7.6035 HZ	
	0.000001	-0.000005	0.000546
	0.002112	-0.003616	0.004531
	0.000004	0.000004	0.005404
	-0.000126	-0.003068	
	-0.000002	0.000002	
	0.000000	0.000000	

MODE = 20	FREQ =	9.7917 HZ	
	0.000098	-0.000271	0.003720
	0.000011	-0.000036	0.010713
	-0.000001	-0.000001	0.011700
	0.000015	-0.000035	
	-0.000136	0.000262	
	0.000002	0.000002	
MODE = 21	FREQ =	9.9097 HZ	
	-0.347569	0.999941	6.283185
	-0.000054	0.000154	0.000000
	0.000000	0.000000	0.000000
	-0.000077	0.000157	
	0.497623	-1.018807	
	0.000000	0.000000	
MODE = 22	FREQ =	9.9102 HZ	
	0.000054	-0.000155	0.000000
	-0.347462	1.000165	0.000000
	0.000000	0.000000	724.752747
	-0.497849	1.018563	
	-0.000077	0.000157	
	0.000000	0.000000	
MODE = 23	FREQ =	10.6229 HZ	
	0.000000	-0.000004	0.000001
	0.000010	-0.000077	0.000000
	-0.000004	-0.000004	0.000000
	0.000013	-0.000061	
	-0.000002	0.000004	
	-0.000000	-0.000000	
MODE = 24			
	-0.000002	0.000031	0.000000
	-0.000000	0.000002	0.000000
	-0.000001	-0.000001	0.000003
	-0.000008	0.000005	
	0.000014	-0.000058	
	0.000004	0.000004	

Combined Model Rigid Body

Properties :

Mass = 9220.0 kg

Center of mass = (0 , 0.81345 , 6.833) m

Inertia Matrix 1212690 0 0
about Mass Center = 0 1279220 -63753 kg(m**2)
 0 -63753 401329

TABLE 6

STRENGTH MODEL MODES OF COMBINED STRUCTURE MODEL
 (zero frequency modes omitted).
 All displacements are in meters.
 Modes are normalized to unity generalized mass.

The following table displays modal displacements. The format is as shown.

	ACTUATOR	SENSOR	LOS MOTION
MODE = N		FREQ =	X.XXXX HZ
X Translation	X•XXXXXX	X•XXXXXX	X•XXXXXX
Y Translation	X•XXXXXX	X•XXXXXX	X•XXXXXX
Z Translation	X•XXXXXX	X•XXXXXX	X•XXXXXX
X Rotation	X•XXXXXX	X•XXXXXX	
Y Rotation	X•XXXXXX	X•XXXXXX	
Z Rotation	X•XXXXXX	X•XXXXXX	
MODE = 1		FREQ =	0.1706 HZ
	-0.004151	0.002514	-0.042006
	-0.001615	-0.001423	-0.063311
	-0.001004	-0.001004	0.000625
	0.000061	0.000211	
	-0.002154	-0.002189	
	0.000085	0.000085	
MODE = 2		FREQ =	0.2342 HZ
	0.000001	0.000198	-0.000001
	0.000080	0.000332	-0.000017
	0.004126	0.004126	0.000733
	0.000080	0.000025	
	-0.000037	-0.000020	
	0.000164	0.000164	
MODE = 3		FREQ =	0.3487 HZ
	0.002358	0.005213	0.004645
	-0.001465	0.000650	-0.347391
	-0.002632	-0.002632	0.000003
	0.000682	0.001872	
	0.001155	0.002432	
	-0.000989	-0.000989	

MODE = 4	FREQ =	0.3816 HZ	
	0.000510	0.001425	0.006990
	0.000775	-0.000984	0.006862
	0.000456	0.000456	0.001338
	-0.000567	-0.001338	
	0.000346	0.000739	
	-0.000005	-0.000005	
MODE = 5	FREQ =	0.3826 HZ	
	-0.000156	-0.000429	-0.002310
	-0.000404	0.000624	-0.001646
	0.000138	0.000138	0.002292
	0.000335	0.000910	
	-0.000104	-0.000226	
	-0.000001	-0.000001	
MODE = 6	FREQ =	0.3967 HZ	
	-0.000031	0.004777	-0.000429
	-0.000244	0.000431	0.000624
	-0.000140	-0.000140	0.000138
	0.000218	0.000497	
	0.000328	0.001428	
	-0.000047	-0.000047	
MODE = 7	FREQ =	0.4120 HZ	
	-0.001448	-0.004361	-0.552454
	0.003489	-0.008700	0.831537
	0.0038	0.003802	0.000625
	-0.003941	-0.009132	
	-0.001318	-0.002693	
	0.001072	0.001072	
MODE = 8	FREQ =	0.4351 HZ	
	0.004185	0.018008	0.000002
	0.008542	-0.031320	-0.000024
	0.005390	0.005390	0.000733
	-0.012899	-0.028668	
	0.005348	0.011262	
	-0.000630	-0.000630	

MODE = 9 FREQ = 0.5001 Hz

-0.063651	-0.832899	-0.013364
0.042160	-0.551320	0.999935
-0.000373	-0.000373	0.000003
-0.193041	-0.404670	
-0.291711	-0.611541	
-0.000021	-0.000021	

MODE = 10 FREQ = 0.5002 Hz

-0.042006	-0.552454	0.006990
-0.063311	0.831537	0.006862
0.000625	0.000625	0.001338
0.291072	0.610114	
-0.193555	-0.405768	
-0.000027	-0.000027	

MODE = 11 FREQ = 0.5426 Hz

0.000219	-0.008563	-0.000045
-0.002005	-0.071448	-0.000078
0.006337	0.006337	-0.000227
-0.022774	-0.047965	
-0.003232	-0.006774	
-0.000066	-0.000066	

MODE = 12 FREQ = 0.6425 Hz

-0.005239	0.022999	0.000000
-0.000241	0.004777	0.000000
0.001141	0.001141	0.000000
0.001626	0.002940	
0.010139	0.020957	
-0.000562	-0.000562	

MODE = 13 FREQ = 1.4667 Hz

0.000020	-0.000022	-0.000429
-0.014161	0.055561	0.000624
-0.001192	-0.001192	0.000138
0.019774	0.033236	
-0.000014	-0.000021	
0.000003	0.000003	

RD-A123 530

ACROSS FIFTEEN (ACTIVE CONTROL OF SPACE STRUCTURES) (U)
CONTROL DYNAMICS CO HUNTSVILLE AL S M SELTZER ET AL.
OCT 82 RADC-TR-82-198 F30602-81-C-0179

2/2

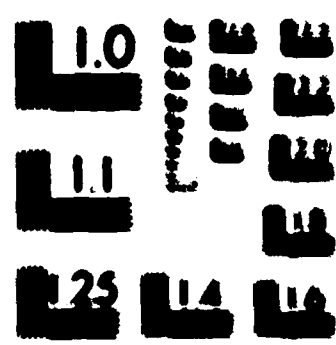
UNCLASSIFIED

F/G 22/2

NL

END

FILMED
10/10/82



1.0
0.1
0.01
25 14

NOTE - 19

Page 1

2000-01

1. 航空機	2. 電動車	3. 汽油車
2. 機械車	3. 機器車	4. 機械車
3. 機械車	4. 機器車	5. 機械車
4. 機械車	5. 機器車	6. 機械車
5. 機械車	6. 機器車	7. 機械車
6. 機械車	7. 機器車	8. 機械車

NOTE - 20

Page 1

2000-01

1. 機械車	2. 機器車	3. 機械車
2. 機械車	3. 機器車	4. 機械車
3. 機械車	4. 機器車	5. 機械車
4. 機械車	5. 機器車	6. 機械車
5. 機械車	6. 機器車	7. 機械車
6. 機械車	7. 機器車	8. 機械車

NOTE - 21

Page 1

2000-01

1. 機械車	2. 機器車	3. 機械車
2. 機械車	3. 機器車	4. 機械車
3. 機械車	4. 機器車	5. 機械車
4. 機械車	5. 機器車	6. 機械車
5. 機械車	6. 機器車	7. 機械車
6. 機械車	7. 機器車	8. 機械車

NOTE - 22

Page 1

2000-01

1. 機械車	2. 機器車	3. 機械車
2. 機械車	3. 機器車	4. 機械車
3. 機械車	4. 機器車	5. 機械車
4. 機械車	5. 機器車	6. 機械車
5. 機械車	6. 機器車	7. 機械車
6. 機械車	7. 機器車	8. 機械車

NOTE - 23

Page 1

2000-01

1. 機械車	2. 機器車	3. 機械車
2. 機械車	3. 機器車	4. 機械車
3. 機械車	4. 機器車	5. 機械車
4. 機械車	5. 機器車	6. 機械車
5. 機械車	6. 機器車	7. 機械車
6. 機械車	7. 機器車	8. 機械車

MODE = 19 FREQ = 3.1337 Hz

0.307536	-0.999649	0.000374
0.666663	-0.013363	0.003162
-0.666663	-0.000000	0.004420
0.666655	-0.013610	
-0.497577	1.018719	
-0.066600	-0.000000	

MODE = 20 FREQ = 3.1339 Hz

0.666663	-0.013364	0.003077
-0.347391	0.999935	0.008950
0.066603	0.000003	0.012950
-0.497858	1.018399	
-0.066651	0.013616	
-0.000000	-0.000000	

MODE = 21 FREQ = 3.7576 Hz

-0.000023	0.000447	6.283185
0.000007	0.000014	0.000000
-0.000003	-0.000003	0.000000
0.000012	0.000006	
0.000187	-0.000024	
0.000055	0.000055	

MODE = 22 FREQ = 9.7914 Hz

-0.000004	-0.000092	0.000010
0.000000	0.000005	0.000000
0.000001	0.000001	724.752747
0.000001	0.000003	
-0.000006	0.000013	
-0.100002	-0.000002	

MODE = 23 FREQ = 10.5475 Hz

0.000001	0.000000	0.000000
0.000003	0.000042	0.000000
0.000004	0.000004	0.000000
0.000004	0.000025	
0.000000	-0.000002	
0.000000	0.000000	

MODE = 24 FREQ = 11.8791 HZ

0.000008	0.000003	0.000000
0.000002	-0.000004	0.000010
-0.000001	-0.000001	0.000011
-0.000006	-0.000000	
0.000000	-0.000028	
0.000004	0.000004	

Combined Model Rigid Body,

Properties :

Mass = 9220.0 kg

Center of mass = (0 , 0.81345 , 6.833) m

Inertia Matrix	1212690	0	0	
about Mass Center =	0	1279220	-63753	kg(m**2)
	0	-63753	401329	

addresses	number of copies
Richard Carman RADC/OCSE	5
RADC/TSLD GRIFFISS AFB NY 13441	1
RADC/DAP GRIFFISS AFB NY 13441	2
ADMINISTRATOR DEF TECH INF CTR ATTN: DTIC-DDA CAMERON STA BG 5 ALEXANDRIA VA 22314	12
Control Dynamics Company 221 East Side Square, Suite 1B Huntsville, AL 35801	5
Charles Stark Draper Labs 555 Technology Square Cambridge, MA 02139	5
Charles Stark Draper Lab Attn: Dr. Keto Soosar 555 Technology Square M.S. -95 Cambridge, MA 02139	1
Charles Stark Draper Lab Attn: Dr. J.B. Linn 555 Technology Square Cambridge, MA 02139	1

Charles Stark Draper Lab
Attn: Mr. R. Strunce
555 Technology Square
M.S.-60
Cambridge, MA 02139

Charles Stark Draper Lab
Attn: Dr. Daniel R. Hogg
555 Technology Square
M.S. -60
Cambridge, MA 02139

ARPA/MIS
1400 Wilson Blvd
Arlington, VA 22209

ARPA/STO
Attn: Lt Col A. Herzberg
1400 Wilson Blvd
Arlington, VA 22209

ARPA/STO
Attn: Maj E. Dietz
1400 Wilson Blvd
Arlington, VA 22209

Riverside Research Institute
Attn. Dr. R. Kappesser
Attn. Mr. A. DeFilliers
1701 N. Ft. Myer Drive Suite 711
Arlington, VA 22209

Riverside Research
Attn: HALO Library, Mr. Bob Pessut
1701 N.Ft. Myer Drive
Arlington, VA 22209

Itek Corp
Optical Systems Division
10 Maguire Rd.
Lexington, MA 02173

Pearlman Communications
Attn: Mr. D. L. Lammertine
Electro Optical Division
Napa Avenue
Nevada, CA 89050

Hughes Aerospace Company
Attn: Mr. George Lewis
R. S. C. 100
Culver City, CA 90230

Hughes Aerospace Company
Attn: Mr. Ron Steele
Concrete Route 1A
Culver City, CA 90230

Air Force Flight Dynamics Lab
Attn: Dr. Lynn Rogers
Wright-Patterson AFB, OH 45433

AIRFLYERS
Attn: Mr. Jerome Pfeffer
Wright-Patterson AFB, OH 45433

Air Force Wright Aero Lab, F-102
Attn: Capt Paul Green
Wright-Patterson AFB, OH 45433

Air Force Institute of Technology
Attn: Prof. R. Collier/DRW
Wright-Patterson AFB, OH 45433

Aerospace Corp.
Attn: Dr. G.T. Young
2350 E. El Segundo Blvd
El Segundo, CA 90245

Aerospace Corp.
Attn: Mr. J. Mastich
2300 E. El Segundo Blvd
El Segundo, CA 90246

Aerospace Corp/81dg 125/1064
Attn: Mr. Steve Burris
Advanced Systems Tech Div.
2300 E El Segundo Blvd
El Segundo, CA 90246

SD/SD/TLVS
Attn: Mr. Lawrence Weeks
P.O. Box 92960
Hollywood Postal Center
Los Angeles CA 90009

SD/YCD
Attn: YCPT/Capt Gajewski
P.O. Box 92960
Hollywood Postal Center
Los Angeles, CA 90009

Grunman Aerospace Corp
Attn: Dr. A. Mandelson
South Oyster Bay Road
Bethpage, NY 11714

OSD/DAS/DS
Attn. Mr. A. Bertapelli
Room 30336
Pentagon, Washington, DC 20301

Jet Propulsion Laboratory
Attn: Mr. D.B. Schoeckter
4800 Oak Grove Drive
Pasadena, CA 91103

MIT/Lincoln Laboratory
Attn: S. Wright
P.O. Box 73
Lexington, MA 02173

MIT/Lincoln Laboratory Attn: Dr. D. Hyland P.O. Box 73 Lexington, MA 02173	11
MIT/Lincoln Laboratory Attn: Dr. N. Smith P.O. Box 73 Lexington, MA 02173	11
Control Dynamics Co. Attn: Dr. Sherman Seltzer 221 East Side Square, Suite 18 Huntsville, AL 35801	1
Lockheed Space Missile Corp. Attn: A. A. Woods, Jr., O/62-E6 p.O. Box 504 Sunnyvale, California 94088-3504	5
Lockheed Missiles Space Co. Attn: Mr. Paul Williamson 3251 Hanover St. Palo Alto, CA 94304	1
General Dynamics Attn: Ray Halstenberg Convair Division 5001 Keary Villa Rd San Diego, CA 92123	1
STI Attn: Mr. R.C. Stroud 20065 Stevens Creek Blvd. Cupertino, CA 95014	1
NASA Langley Research Ctr Dr. Earle K Huckins III Attn: Dr. Card Langley Station Bldg 1293B M/s 230 Hampton, VA 23665	2

NASA Johnson Space Center Attn: Robert Piland Ms. EA Houston, TX 77058	1
McDonald Douglas Corp Attn: Mr. Read Johnson Douglas Missile Space Systems Div 5301 Bulsa Ave Huntington Beach, CA 92607	1
Integrated Systems Inc. Attn: Dr.N. K. Gupta and M.G. Lyons 151 University Avenue, Suite 400 Palo Alto, California 94301	2
Boeing Aerospace Company Attn: Mr. Leo Cline P.O. Box 3999 Seattle, WA 98124 MS 8 W-23	1
TRW Defense Space Sys Group Inc. Attn: Ralph Iwens Bldg 82/2054 One Space Park Redondo Beach, CA 90278	1
TRW Attn: Mr. Len Pincus Bldg R-5, Room 2031 Redondo Beach, CA 90278	1
Department of the navy Attn: Dr. K.T. Alfriend Naval Research Laboratory Code 7920 Washington, DC 20375	1
Airesearch Manuf. Co. of Calif. Attn: Mr. Oscar Buchmann 2525 West 190th St. Torrance, CA 90509	1
Analytic Decisions, Inc. Attn: Mr. Gary Glaser 1401 Wilson Blv. Arlington, VA 22209	1

Ford Aerospace & Communications Corp.
Drs. I. P. Lefebvre and P. Barba, MS/CMS
3939 Fabian way
Palo Alto, California 94304

Center for Analysis
Attn: Mr. Jim Justice
13 Corporate Plaza
Newport Beach, CA 92660

General Research Corp.
Attn: Mr. G. R. Curry
P.O. Box 3587
Santa Barbara, CA 93105

General Research Corp
Attn: Mr. Thomas Zatkowski
7655 Old Springhouse Road
McLean, VA 22101

Institute of Defense Analysis
Attn: Dr. Hans Wolfhard
400 Army Navy Drive
Arlington, VA 22202

Karman Sciences Corp.
Attn: Dr. Walter E. Ware
1500 Garden of the Gods Road
P.O. Box 7463
Colorado Springs, CO 80933

MRJ, Inc.
10400 Eaton Place
Suite 300
Fairfax, VA 22030

Photon Research Associates
ATTN: Mr. Jim Ryan
P.O. Box 1318
La Jolla, CA 92038

Rockwell International
ATTN: Russell Lafferty (Space Systems Group)
Flight Code - 96-501
12214 Lakewood Blvd.
Downey, CA 90241

Defense Applications, Inc.
ATTN: Mr. Richard Ryan
3 Preston Court
Southport, NC 27879

U.S. Army Strategic Command
ATTN: DRBSC-RMS/MR Space Test
Redstone Arsenal, AL

Rockwell Electronic Systems Command
ATTN: Mr. Charles Bond
PMC 100-4
National Center I
Washington, DC 20330

Lockheed Palo Alto Research Laboratory
ATTN: Dr. J. D. Anderson, 6/52-55
3251 Hanover Street
Palo Alto, California 94303-1107

U.S. Army/DARPA
ATTN: Mr. Dennis Chastain
ARC 0104
5001 Eisenhower Ave
Alexandria, VA 22333

Defense Documentation Center
Cameron Station
Alexandria, VA 22314

Honeywell Inc.
Attn: Dr. Thomas B. Cunningham
Attn: Dr. Michael F. Barrett
2600 Ridgway Parkway MN 17-2375
Minneapolis, MN 55413

2

NASA Marshal Space Flight Center
Attn: Dr. J.C. Blair EDOI
Henry B. Waites
Marshal Space Flight Center AL 35812

2

MISSION
of
Rome Air Development Center

RADC plans and executes research, development, test and selected acquisition programs in support of Command, Control, Communications and Intelligence (C3I) activities. Technical and engineering support within areas of technical competence is provided to ESD Program Offices (POs) and other ESD elements. The principal technical mission areas are communications, electromagnetic guidance and control, surveillance of ground and aerospace objects, intelligence data collection and handling, information system technology, ionospheric propagation, solid state science, microwave physics and electronic reliability, maintainability and compatibility.